

TITLE

Exceeding 1.5°C global warming could trigger multiple climate tipping points.

AUTHORS

Armstrong McKay, DI; Staal, A; Abrams, JF; et al.

JOURNAL

Science

DEPOSITED IN ORE

03 November 2022

This version available at

<http://hdl.handle.net/10871/131584>

COPYRIGHT AND REUSE

Open Research Exeter makes this work available in accordance with publisher policies.

A NOTE ON VERSIONS

The version presented here may differ from the published version. If citing, you are advised to consult the published version for pagination, volume/issue and date of publication

Title: Updated assessment suggests >1.5°C global warming could trigger multiple climate tipping points

Authors: David I. Armstrong M^cKay^{1,2,3*†}, Arie Staal^{1,2,4}, Jesse F. Abrams³, Ricarda Winkelmann⁵, Boris Sakschewski⁵, Sina Loriani⁵, Ingo Fetzer^{1,2}, Sarah E. Cornell^{1,2}, Johan Rockström^{1,5}, Timothy M. Lenton^{3*}

Affiliations:

¹ Stockholm Resilience Centre, Stockholm University; Stockholm, Sweden.

² Bolin Centre for Climate Research, Stockholm University; Stockholm, Sweden.

³ Global Systems Institute, University of Exeter; Exeter, UK.

⁴ Copernicus Institute of Sustainable Development, Utrecht University; Utrecht, Netherlands.

⁵ Potsdam Institute for Climate Impact Research; Potsdam, Germany.

*david.armstrongmckay@su.se / d.mckay@exeter.ac.uk, t.m.lenton@exeter.ac.uk

† Current address: Georesilience Analytics; Leatherhead, UK.

Short title:

Reassessment of climate tipping elements

Keywords:

Climate change; climate tipping elements; tipping points; climate feedbacks; abrupt change; nonlinear dynamics

This paper is a non-peer reviewed preprint submitted to Science for review.

Abstract: Climate tipping points occur when change in a part of the climate system becomes self-perpetuating beyond a forcing threshold, leading to abrupt and/or irreversible impacts. Synthesizing paleoclimate, observational, and model-based studies, we provide a revised shortlist of global ‘core’ tipping elements and regional ‘impact’ tipping elements and their temperature thresholds. Current global warming of $\sim 1.1^\circ\text{C}$ above pre-industrial already lies within the lower end of some tipping point uncertainty ranges. Several more tipping points may be triggered in the Paris Agreement range of $1.5\text{-}2^\circ\text{C}$ global warming, with many more likely at the $2\text{-}3^\circ\text{C}$ of warming expected on current policy trajectories. This strengthens the evidence base for urgent action to mitigate climate change and to develop improved tipping point risk assessment, early warning capability, and adaptation strategies.

One-sentence summary: New categorization and synthesis of climate tipping point estimates strengthens evidence to limit global warming to 1.5°C .

Main Text:

Since (1) climate tipping points (CTPs) have emerged as a growing research topic and source of public concern (2, 3). Tipping points were defined as “*a critical threshold at which a tiny perturbation can qualitatively alter the state or development of a system*” (1). Several large-scale Earth system components, termed “tipping elements”, were identified with evidence for tipping points that could be triggered by human activities this century. The initial shortlist comprised: Arctic summer sea-ice, Greenland ice sheet (GrIS), West Antarctic ice sheet (WAIS), Atlantic Meridional Overturning Circulation (AMOC; then labelled THC), El Niño Southern Oscillation, Indian Summer monsoon, Sahara/Sahel and West African Monsoon, Amazon rainforest, and boreal forest. Literature review (1) and a corresponding expert elicitation (4) provided early estimates of their temperature thresholds and potential interactions. Subsequent work showed how recognition of CTPs significantly affects risk analysis and supports measures to minimize global warming to the Paris Target of 1.5°C (5, 6).

Since (1) there have been considerable advances in our knowledge of CTPs, from observations of nonlinear changes in the climate system, statistical early warning methods, palaeoclimate evidence, upgraded Earth system models (ESMs), and improved offline models of particular elements (e.g. ice sheets and vegetation). Notably, observations and models suggest parts of the WAIS may be approaching (7, 8) or even have passed a tipping point (9, 10). Early warning indicators have revealed destabilization of parts of the GrIS and the AMOC (11, 12). However, many ESMs still lack processes important for resolving potential tipping behavior, e.g. being biased towards AMOC stability (13), or underestimating current tropical carbon sink decline (14). Potential causal interactions among tipping elements (4) are such that overall tipping one element increases the likelihood of tipping others (15), risking a ‘tipping cascade’ of impacts that may also amplify global warming (2, 3). In the worst case, interactions might produce a global CTP (3).

The list of tipping elements has evolved over time (1–3, 5) (Supplementary Table S1). Different studies have proposed potential additions including: southwest North America, the Yedoma permafrost region, the North Atlantic subpolar gyre (16); low-latitude coral reefs, the East Antarctic Ice Sheet (EAIS), Arctic Winter Sea Ice (AWSI), Alpine glaciers (5); the northern polar jet stream (3); the Congo rainforest (17); and the Wilkes and Aurora sub-glacial basins in East Antarctica (2). A range of abrupt shifts have been identified in CMIP5 models (18), some in elements not on the original shortlist, such as boreal tundra or Antarctic sea-ice. Conversely, Arctic summer sea-ice (19, 20), ENSO (21, 22), and monsoons (23) have been argued not to be CTPs. Numerous temperature threshold estimates have been made since (1), with some being revised markedly downwards – notably WAIS (2, 24). The recent IPCC AR6 WG1 report identified up to 15 candidates (Table 4.10), but was not explicit about their temperature thresholds (22).

Here we reassess the climate tipping elements based on the substantial literature published since (1), focusing on those triggerable by global warming. We clarify the definition of tipping elements and points and propose a new categorization separating global ‘core’ and regional ‘impact’ tipping elements. Then we provide an updated list and assessment of the global mean surface temperature (GMST) range at

which each candidate CTP could occur as well as their timescales and climate impacts. Finally, we combine this information to assess the likelihood of triggering CTPs at successive global warming levels.

Defining tipping points and tipping elements

In a world of multiple inconsistent definitions of a CTP, we anchor on the technical definition provided by (1): a tipping point is a critical point in a (forcing) ‘control parameter’ at which a small additional perturbation causes a qualitative change in the future state of a system after some observation time. More informally: tipping points occur when change in a part of the climate system becomes self-perpetuating beyond a forcing threshold, leading to difficult to reverse nonlinear impacts. We now explain key aspects of this definition in more detail.

Self-perpetuating change. Self-perpetuation mechanisms are critical to the existence of a tipping point (also termed a ‘critical point’ or ‘threshold’) in a system, beyond which they propel qualitative change (a ‘regime shift’), such that even if forcing of the system ceases qualitative change continues to unfold regardless (19). Self-perpetuation is usually due to positive feedback within a system getting sufficiently strong to (temporarily) reach the ‘runaway’ condition (where an initial change propagating around a feedback loop gives rise to an additional change that is at least as large as the initial change, and so on). Most positive feedbacks never attain this condition and instead simply amplify the original driver in a constrained way. Notably, Arctic summer sea ice loss involves the positive ice-albedo feedback, but (unlike year-round sea ice loss) that feedback is not strong enough alone to produce a clear threshold beyond which loss would continue even if global warming stopped (19, 20). Consequently, we describe such feedbacks as ‘threshold-free’.

(Ir)reversibility. Tipping points can lead to reversible or irreversible qualitative change (1) (depending on the type of underlying mathematical bifurcation). Other definitions of CTPs are more restrictive, requiring irreversibility, e.g.: “*a system reorganizes... and does not return to the initial state even if the drivers of the change are abated*” (6.1.1 of (21)). The IPCC AR6 does not require irreversibility: “A

tipping point is a critical threshold beyond which a system reorganizes, often abruptly and/or irreversibly” (4.7.2 of (22)). However, in practice AR6 applies stricter criteria, ruling out particular candidate CTPs on grounds of lack of abruptness (e.g. GrIS) or lack of irreversibility (e.g. Arctic sea ice, and Box 12.1 Table 1 of (25)). We aim to be more consistent with the AR6 definition.

Timescale and abruptness. We allow for CTPs (e.g. in ice sheets) where the resulting qualitative change is slower than the anthropogenic forcing causing it, i.e. not ‘abrupt’ in the sense defined as “*faster than the cause*” (26). We only require that the “*transition to a new state*” occurs “*at a rate determined by the climate [sub-]system itself*” (26). Resulting committed (often irreversible) qualitative changes can unfold over centuries to millennia (here we relax our ‘ethical’ time horizon (*I*) to ~10kyr), but crucially they can increase short-term impacts (e.g. rate of sea level rise). Others require a tipping point to produce abrupt change (27), thereby excluding e.g. ice sheet collapse. IPCC gives a different, purely timescale-based definition of abrupt climate change, as taking place “*over a few decades or less*” and persisting “*for at least a few decades*” (28). Such changes could simply be due to an abrupt change in forcing without involving CTPs. Over a dozen abrupt changes have been found in CMIP5 model output (18). Below we assess which are potential tipping elements (and which do not involve self-perpetuating feedback; Supplementary Table S2).

Spatial scale. Tipping elements are defined as at least sub-continental scale, $O(1000\text{km})$, components of the Earth system that could pass a tipping point due to actions this century (*I*). If self-perpetuating change (and a corresponding tipping point) occurs at sub-continental scale then this qualifies as a global ‘core’ tipping element. However, there are many examples of runaway feedback and associated tipping points at smaller spatial scales. Where a change in forcing, e.g. temperature, is fairly uniform across a large spatial scale, such that a smaller-scale tipping point is crossed near-synchronously in many locations that span a sub-continental scale (e.g. coral bleaching across the Great Barrier Reef, or melt of Himalayan glaciers), then these are considered potential regional ‘impact’ tipping elements. Where systems exhibit localized tipping points (1m-1km) at different forcing levels such that change does not self-perpetuate beyond a

clear shared threshold (e.g. methane hydrates), these are classed as ‘threshold-free’ feedbacks – because the accumulated global consequences of multiple localized tipping events remains roughly proportional to the forcing.

Impacts. Tipping elements either: (i) contribute significantly to the overall mode of operation of the Earth system (such that tipping them modifies the overall state of the whole system); (ii) contribute significantly to human welfare (such that tipping them impacts on $>\sim 100$ million people), or; (iii) have great value in themselves as a unique feature of the Earth system (expanded from ‘biosphere’ in (1)). Global ‘core’ tipping elements must meet criterion (i), whereas regional ‘impact’ tipping elements meet criterion (ii) or (iii) but not (i). Regarding (i), crossing a tipping point need not involve feedback to global atmospheric composition or temperature – self-perpetuating feedback can be purely within a tipping element (1) – but there is usually causal coupling to other tipping elements – e.g. via heat, salt, water, carbon, or momentum fluxes (4). Often there is feedback to global warming, and where this exceeds 0.1°C (i.e. natural variability) we consider this to meet criterion (i). Thus, near-synchronous, large-scale crossing of smaller-scale tipping points can qualify as a global ‘core’ tipping element if it amplifies warming by $>0.1^{\circ}\text{C}$.

The Climate Tipping Elements

Based on current observations, palaeo-records, and model runs subsequent to (1), we draw up a longlist of proposed climate tipping elements. Together with expert judgment for each, we summarize the evidence and confidence levels for self-perpetuation, temperature thresholds, hysteresis / irreversibility, transition timescales, and global / regional impacts on climate (Supplementary Table S3). Based on this evidence and the definitions in Section 2, we shortlist Global ‘Core’ and Regional ‘Impact’ climate tipping elements (Table 1; Fig. 1). Other candidate tipping elements that we consider uncertain, unlikely, or threshold-free feedbacks are discussed in the Supplementary Text, together with differences to past assessments (Supplementary Table S4).

[Table 1]

[Fig. 1]

Cryosphere

Arctic sea-ice (ASSI/AWSI/BARI). Arctic summer sea ice (ASSI) has been declining rapidly since the 1970s in linear response to cumulative emissions, outpacing past IPCC projections since the 1990s (29). This decline is amplified by the ice-albedo feedback, and possibly feedbacks to cloud cover, but damped by negative heat loss feedbacks (19). CMIP6 models better capture historical ASSI decline, and project occasional ice-free Septembers will occur above 1.5°C GMST, becoming common beyond 2°C, and permanent around 3°C (30). However, the linearity of the modelled and observed responses suggest that it is unlikely to feature a tipping point beyond which loss would self-perpetuate (20, 30). Hence, we re-categorize ASSI as a threshold-free feedback. In contrast, an abrupt collapse in Arctic winter sea ice (AWSI) (31) is observed in some CMIP5 models beyond ~4.5°C (18, 32) which arises either from asymmetry in ice formation and loss timescales creating a threshold response or from local positive feedback cycles. Hence we class AWSI as a global core tipping element [medium confidence], with a best estimate threshold of ~6.3°C (4.5-8.7°C, based on CMIP5) [high confidence], timescales of 20y (10-100y) [high confidence], and GMST feedback of ~+0.6°C (~+0.25°C when summer ice-free; regional ~+0.6-1.2°C) [high confidence]. A sub-case is abrupt loss of Barents Sea winter ice (BARI), which occurs at ~1.6°C in two CMIP5 models (18), is self-reinforced by an increased inflow of warm Atlantic waters (33), and has significant impacts on atmospheric circulation, European climate, and potentially the AMOC (34). We consider BARI a probable regional impact tipping element [medium confidence] with a threshold of 1.6°C (1.5-1.7°C) [medium confidence], timescale of ~25y [medium confidence], and regional warming [low confidence].

Greenland ice sheet (GrIS). The GrIS is shrinking at an accelerating rate due to both net surface melt and accelerated calving (35, 36), and shows early warning signals consistent with the approach to a

tipping point in west Greenland (11). Both ice sheet modelling and palaeoclimate data indicate a GrIS tipping point can occur when the melt-elevation feedback gets strong enough to support self-propelling melt (as ice sheet surface loses height it enters warmer air and thus melts faster) (1). Different models give a critical threshold of $\sim 1.6^{\circ}\text{C}$ ($0.8\text{--}3.2^{\circ}\text{C}$) (37), $\sim 1.5^{\circ}\text{C}$ (38) or $2.7 \pm 0.2^{\circ}\text{C}$ (39). Palaeoclimate and model evidence shows ice only reaching full coverage below $\sim 0.3\text{--}0.5^{\circ}\text{C}$ ($\sim 300\text{ppm CO}_2$) (37, 40). Hysteresis allows GrIS to exist above this growth threshold once formed (37), but palaeorecords indicate that GrIS partially retreats above this threshold (40) and likely collapsed during the long $>1.5^{\circ}\text{C}$ warmer MIS-11 interglacial (41). A coupled ice sheet-atmosphere model found no collapse threshold (42), leading AR6 to state there is limited evidence for irreversible GrIS loss below 3°C (20). However, some irreversible loss occurs beyond 3.5m sea level equivalent (equivalent to $\sim 2\text{--}2.5^{\circ}\text{C}$) (42), indicating self-perpetuating feedback. GrIS collapse would shift the Earth system to a unipolar icehouse state and impact other tipping elements (in particular the AMOC), hence qualifying as a global core tipping element [medium confidence]. Our best estimates for GrIS is a threshold of $\sim 1.5^{\circ}\text{C}$ ($0.8\text{--}3^{\circ}\text{C}$) [medium confidence], timescales of 10ky (1ky-15ky) [medium confidence], and GMST feedback of $\sim +0.13^{\circ}\text{C}$ (regional $\sim +0.5\text{--}3^{\circ}\text{C}$) [medium confidence]. The timescale of ice sheet meltdown gets shorter the greater the temperature threshold is exceeded (38), with a minimum of $\sim 1000\text{y}$.

West Antarctic ice sheet (WAIS). Large parts of the WAIS are grounded below sea level – if the grounding line in these marine ice-sheet basins reaches retrograde slopes, this can lead to the onset of the Marine Ice Sheet Instability (MISI) and crossing of a tipping point (7, 8, 43). MISI is based on a feedback between the grounding line retreat and ice flux across the grounding line as it reaches thicker ice. This can lead to self-sustaining retreat, and is hypothesized to have driven past collapses of the WAIS during past warmer interglacial periods with high sea levels (20, 44). Some glaciers in the Amundsen Sea Embayment are already close to this threshold, and experiencing significant grounding line retreat (9). Thwaites glacier's grounding line is only $\sim 30\text{km}$ away from the subglacial ridge and retreating at $\sim 1\text{km/year}$ (45) and eventual collapse may already be inevitable (10, 43). Models support irreversible

retreat being underway for present levels of ocean warming (24, 46), and suggest that losing Thwaites glacier can destabilize much of WAIS (7). Under sustained 1°C warming one model shows partial WAIS collapse with mass loss peaking at ~2°C warming (24). Hence, we retain WAIS as a core global tipping element [high confidence], with a best estimate threshold of ~1.5°C (1-3°C, down from 3.5-5.5°C in (1)) [high confidence], timescales of 2ky (500y-13ky) [medium confidence], and GMST feedback of ~+0.05°C (regional ~+1°C) [medium confidence]. Higher threshold exceedance reduces transition timescale to a minimum of ~500y (38).

East Antarctic sub-glacial basins (EASB). Recent data and models have shown that several subglacial basins of the East Antarctic ice sheet (EAIS) – in particular the Wilkes, Aurora, and Recovery Basins – are also affected by MISI (24, 47). Likewise they may also be subject to ‘marine ice cliff instability’ (MICI) in which the collapse of floating ice shelves creates unstable ice cliffs at the marine edge of the ice sheet that can retreat faster, but the significance of this process is disputed (47, 48). One model indicates that Wilkes collapse may be committed by 3-4°C (24). Palaeoclimate evidence for mid-Pliocene sea level being 5-25m higher indicates that parts of the EASB (together with the GrIS and WAIS), were likely absent in that ~2.5-4°C warmer world (20, 40, 49). In contrast, sea levels of +6-13m at 1.1-2.1°C in MIS-11 does not require significant EASB contribution (assuming WAIS and GrIS were lost) (50). Hence we class EASB as a core global tipping element [high confidence] with best estimates for a tipping threshold of 3°C (2-6°C) [medium confidence], timescales of 2ky (500y-10ky) [medium confidence], and an uncertain GMST feedback provisionally assumed to be similar to WAIS (i.e. ~+0.05°C) [low confidence].

East Antarctic ice sheet (EAIS). The land-grounded bulk of the EAIS is the world’s largest ice sheet, containing the equivalent of ~50m of sea level potential (24). Palaeorecords indicate it grew once atmospheric CO₂ fell below ~650-1000 ppm (~6-9°C) (40). Modelled ice sheets often exhibit alternative ice-covered or ice-free stable states for a range of global boundary conditions (51). Due to this hysteresis, the EAIS is expected to remain stable some way beyond 650ppm, and survived through the warm mid-

Miocene Climatic Optimum ~16 Mya (~2-4°C) (40). However, long-term stabilization at ~1000+ppm CO₂ and ~8-10°C warming could cause total disintegration (24). Once past this threshold, self-perpetuating feedbacks amplify ice loss (37). The loss of EAIS would have global effects, hence is categorized as a global core tipping element [medium confidence]. Although unlikely, under high emissions (e.g. RCP8.5) and high climate sensitivity it might conceivably be committed to this century. Our best estimates for the EAIS are a tipping threshold of ~7.5°C (5-10°C) [high confidence], timescales of >10ky (10k-100ky) [medium confidence], and GMST feedback of ~+0.6°C (regional ~+2°C) [medium confidence].

Boreal permafrost (PFTP/PFAT/PFGT). Permanently frozen soils and sediments in the boreal region contain ~1035 GtC that can be partly released as CO₂ and methane upon thawing (52). Although initially lacking of evidence for a synchronous large-scale threshold (1), subsequent assessments recognized part(s) of the permafrost could be a tipping element (3, 16). Here we separate permafrost into three components with different dynamics: gradual thaw (PFGT; a threshold-free feedback [high confidence]); abrupt thaw (PFAT; a regional impact tipping element [medium confidence]), and; collapse (PFTP: a global core tipping element [low confidence]). Gradual permafrost thaw (PFGT) is observed in modern and palaeorecords beyond 1-1.5°C and in several models acts as a potentially nonlinear but threshold-free feedback (52–54) (see SM). Abrupt thaw processes (PFAT) such as slope slumping and thermokarst lake formation (52) could increase emissions by 50-100% (55), involve localized tipping dynamics (e.g. continued thaw subsidence after initiation), and could occur near synchronously on a sub-continental scale. Our best estimates for PFAT are a tipping threshold of 1.5°C (1-2.3°C) [high confidence], timescale of 200y (100-300y) [medium confidence], and an additional ~25-50% emissions beyond gradual thaw (~13-25 GtC per °C). Finally, abrupt permafrost drying at ~4°C (56), and/or sufficiently rapid regional warming (>9°C) corresponding to ~5°C globally (16, 57) could act as a trigger for permafrost collapse (PFTP) driven by internal heat production in carbon-rich permafrost – the ‘compost bomb’ instability (58, 59). The Yedoma deep ice- and carbon-rich permafrost (containing ~115 GtC in Yedoma deposits, ~400

GtC across Yedoma domain) is particularly vulnerable, as fast thaw processes can expose previously isolated deep deposits (52, 57). This and other regions vulnerable to abrupt drying at $>4^{\circ}\text{C}$ (56) could have significant feedback to global temperature. Our best estimates for PFTP is a threshold of 4°C (3- 6°C) [low confidence], timescale of 50y (25-100y) [medium confidence], and emissions on the order of ~ 264 GtC ($\Delta\text{GMST} \sim +0.3\text{-}0.4^{\circ}\text{C}$) [low confidence].

Extra-polar mountain glaciers (GLCR). Lower-latitude alpine glaciers have individual mass balance thresholds and elevation feedbacks, yet large-scale synchronous losses are projected in several key regions at specific global warming levels. In transient simulations, ‘Peak Water’ from European glacier melt is expected at $\sim 1^{\circ}\text{C}$ (60) with near-total loss expected to be committed at $\sim 2^{\circ}\text{C}$ (19). Global Peak Water occurs at $\sim 2^{\circ}\text{C}$, but committed eventual loss is expected at lower temperatures (61). Long model integrations show that global warming of $1.5\text{-}2^{\circ}\text{C}$ is sufficient to lead to the eventual loss of most extra-polar glaciers (and possibly even polar glaciers) (38, 62). RCP4.5 ($>2^{\circ}\text{C}$ by 2100) puts most lower-latitude glaciers on a path to significant losses beyond 2100 (20). Glaciers in High Mountain Asia last longer than elsewhere, but reach peak water at $\sim 2^{\circ}\text{C}$ with significant social impacts for South Asia (60). Given the considerable human impacts of glacier loss (61), we categorize lower-latitude mountain glaciers as a regional impact tipping element [medium confidence]. Our best estimate is a threshold of $\sim 2^{\circ}\text{C}$ ($1.5\text{-}3^{\circ}\text{C}$) [medium confidence], timescale of 200y (50y-1ky) [medium confidence], and GMST feedback of $\sim +0.08^{\circ}\text{C}$ (regionally greater) [medium confidence].

Southern Ocean sea-ice features abrupt events in some climate models (18), but due to uncertain dynamics and low confidence in projections is classed as an uncertain tipping element (see SM). **Marine methane hydrates** are classed as a threshold-free feedback and **Tibetan plateau snow** as uncertain (see SM).

Ocean-Atmosphere (circulation)

North Atlantic sub-polar gyre / Labrador Sea convection (LABC). Convection in the Labrador Sea in the North-west Atlantic – part of the sub-polar gyre (SPG) – abruptly collapses in some models as a result of warming-induced stratification, a state which is then maintained by self-reinforcing convection feedbacks (18, 63) giving two alternative stable states with or without deep convection. Abrupt future SPG collapse occurs in nine runs across five CMIP5 models at 1.1-2.0°C, and in one additional model run at 3.8°C (18, 63), and in four CMIP6 models in the 2040s (~1-2°C) (64). In some models SPG collapse affects AMOC strength, but SPG and AMOC have distinct feedback dynamics, patterns of impacts, and SPG collapse can occur much faster than AMOC collapse. SPG collapse causes a concentrated North Atlantic regional cooling of ~2-3°C, global cooling of ~0.5°C, a northward-shifted jet stream, weather extremes in Europe, and southward shift of the intertropical convergence zone (ITCZ) (63, 64). Given clear tipping dynamics and global impact we class SPG as a global core tipping element [medium confidence], with a best estimate threshold of ~1.8°C (1.1-3.8°C) [high confidence], timescale of 10y (5-50y) [high confidence], and GMST feedback of ~0.46°C (regional ~-3°C) [medium confidence].

Atlantic meridional overturning circulation (AMOC). The AMOC is self-sustaining due to salt-advection feedback (northward movement of warm water increases its density due to cooling and evaporation supporting the deep convection that drives the circulation). Import of salt at the southern boundary of the Atlantic also supports alternative ‘strong’ and ‘weak’ AMOC stable states, with multiple abrupt switches between them observed in the past (65). Global warming increases Arctic precipitation, freshwater runoff from Greenland, and sea surface temperatures, slowing down the AMOC by inhibiting deep convection. The AMOC has weakened an estimated ~15% over the last ~50 years (66) and early warning signals are consistent with the current AMOC ‘strong’ state losing stability (12). Yet the IPCC gives *low confidence* on historical AMOC trends (20), and assess AMOC collapse *occurring* during the 21st century to be “very unlikely, but physically plausible” in SROCC (21) and unlikely (*medium confidence*) in AR6 (20). However, AMOC collapse is *triggered* in three runs of one CMIP5 model at 1.4-1.9°C and in two runs of an additional model at 2.2-2.5°C (18, 63). Furthermore, IPCC models are

generally biased towards stability with respect to observational constraints (13) and do not consider sensitivity to rate of ice melt (20, 67), both factors making AMOC more vulnerable to collapse. AMOC collapse would have global impacts on temperature and precipitation patterns, including North Atlantic cooling, Southern Hemisphere warming, southward-shifted ITCZ, monsoon weakening in Africa and Asia and strengthening in Southern Hemisphere leading to drying in Sahel and parts of Amazonia, and reduced natural carbon sinks (68–71). Hence, AMOC is retained as a core global tipping element [medium confidence] with best estimate threshold of $\sim 4^{\circ}\text{C}$ ($1.4\text{--}8^{\circ}\text{C}$, vs. $3.5\text{--}5.5^{\circ}\text{C}$ in (1)) [low confidence], timescales of $\sim 100\text{y}$ ($15\text{--}300\text{y}$) [medium confidence], and a GMST feedback of -0.54°C (regional -4 to -10°C , highly heterogeneous global pattern) [medium confidence].

The **Indian summer monsoon** (and other monsoon systems) is reclassified as an uncertain climate tipping element because of a lack of evidence for a warming-related threshold behavior. **Equatorial stratocumulus cloud breakup** and **Indian Ocean upwelling** are uncertain, due to limited evidence. **Global ocean anoxia** is uncertain because the global warming level required for weathering-induced anoxia is unclear. The **El Nino Southern Oscillation** is reclassified as unlikely to be a tipping element, because it lacks a clear self-perpetuation threshold. **Arctic ozone hole expansion** is reclassified as unlikely because it is now unlikely to be triggerable due to climate change. The **Northern Polar Jet stream** is classed unlikely because instability as a result of climate change remains uncertain and no threshold has been proposed. (All are discussed in the SM.)

Biosphere

Amazon rainforest (AMAZ). The Amazon forest biome stores ~150-200 GtC (3, 72, 73) and historically has been a strong sink for human CO₂ emissions (14). This sink has declined since the 1990s though (14), while a combination of a climate change-induced drying trend, unprecedented droughts, and anthropogenic degradation in the south and east has led to the biome as a whole becoming a net carbon source (72). Rainfall is projected to further decline and the dry season to lengthen in southern and eastern areas of the forest with further warming, likely worsening this trend (73). ~17% of the Amazon forest has been lost to deforestation since the 1970s, and deforestation has accelerated since 2019 (73). The Amazon forest recycles around a third of the Amazon basin's rainfall on average (74) and up to ~70% in parts of the basin (75), particularly during the critical dry season as the forest maintains transpiration fluxes (80). This and localized fire feedbacks mean ~40% of the Amazon forest is estimated to currently be in a bi-stable state, increasing to ~66% on a RCP8.5 trajectory (17, 75), and rainforest loss could initiate self-reinforcing drying that tip this portion into a degraded or savannah-like state. Widespread 'Amazon dieback' was originally projected at either 3-4°C of warming or ~40% deforestation (76), but uncertain synergistic interaction might bring the deforestation threshold to only ~20-25% (77). More recent ESMs tend not to simulate climate-induced Amazon dieback and emergent constraints indicate lower rainforest sensitivity to warming (78). However, two CMIP5 models exhibit dieback at 2.5°C and 6.2°C (18), and CMIP5 ESMs underestimate observed tree mortality (14) and likely overestimate CO₂ fertilization (79), potentially making these models under-sensitive to dieback. Given the size of the region affected by even partial dieback, and its global impacts, we categorize the Amazon forest as a global core tipping element [medium confidence]. Our best estimates for AMAZ are a threshold of ~3.5°C (2-6°C) independent of deforestation (and likely lower with deforestation) [medium confidence], timescales of 100y (50-200y) [medium confidence], and partial dieback (40%, i.e. currently bistable area) leading to emissions of ~30 GtC and along with biogeophysical feedbacks (see SM) to a GMST feedback of ~0.06° (regional +1-2°C) [medium confidence].

Boreal forest (BORF/TUND). The Boreal forest (or ‘Taiga’) encircling the Arctic region features multiple stable states of tree cover as a result of feedbacks including albedo and fire (80, 81). We classify it as a regional impact tipping element with two potential CTPs associated with abrupt dieback at its southern edge (BORF) [medium confidence] and abrupt expansion at its northern edge (tundra greening) (TUND) [medium confidence]. Warming is projected to destabilize the southern edge, where factors like hydrological changes, increased fire frequency, and bark beetle outbreaks can lead to self-reinforcing feedbacks driving regionally synchronized forest dieback [O(100km)] to a grass-dominated steppe/prairie state. Models project regime shifts starting in this area at $\sim 1.5^{\circ}\text{C}$ and becoming widespread by $>3.5^{\circ}\text{C}$ (82, 83). Dieback may also be rate-dependent (83). Our best estimates for BORF is a threshold of $\sim 4^{\circ}\text{C}$ ($1.4\text{--}5^{\circ}\text{C}$) [low confidence], timescales of 50y (25-100y) [low confidence], and partial ($\sim 50\%$) dieback leading to emissions of ~ 52 GtC, which along with countervailing biogeophysical feedbacks (increased albedo, reduced evapotranspiration) leads to a net GMST feedback of $\sim -0.08^{\circ}\text{C}$ (regional $\sim -1^{\circ}\text{C}$) [mid confidence]. Northward expansion of the forest into the current tundra biome may also feature self-perpetuation dynamics, e.g. by causing further local warming via albedo feedback. Models suggest regime shifts begin in this northern area at $\sim 1.5^{\circ}\text{C}$ and become widespread by $\sim 3.5^{\circ}\text{C}$ (82), with abrupt high latitude forest expansion occurring in one CMIP5 model at 7.2°C (18). For TUND our best estimates are for a threshold at $\sim 4^{\circ}\text{C}$ ($1.5\text{--}7.2^{\circ}\text{C}$) [low confidence], timescales of 50y (40-100y) [medium confidence], and partial ($\sim 50\%$) uptake of 31 GtC which along with countervailing biogeophysical feedbacks (decreased albedo, increased evapotranspiration) leads to a net GMST feedback of $+0.08^{\circ}\text{C}$ per $^{\circ}\text{C}$ (regional $\sim +1^{\circ}\text{C}$) [medium confidence].

Sahel vegetation & the West African monsoon (SAHL). Palaeo-evidence indicates multiple abrupt shifts into and out of African Humid Periods with associated greening of the Sahara, in response to gradual changes in orbital forcing (84). AMOC weakening and associated warming of the Equatorial East Atlantic also caused past collapses of the West African monsoon (WAM) (68, 84, 85). Dust aerosol-rainfall positive feedbacks amplify change, alongside well-established vegetation-rainfall positive

feedbacks, but many models still underestimate self-amplifying feedbacks because they cannot reproduce the extent of past rainfall and vegetation changes (84). In contrast, a model optimized against present observations and mid-Holocene reconstructions recently reproduced abrupt transitions in Saharan vegetation (86). In future projections with GHG forcing, global (CMIP5, CMIP6) and some regional (CORDEX) climate models tend to predict strengthening of the WAM, wetting [and northward expansion] of the central and eastern Sahel (and drying in coastal west Africa) (22, 68, 87–89), which would tend to green the Sahel (84). Abrupt increases in vegetation in the Eastern Sahel occur in three ESM runs at 2.1–3.5°C (18). In other global models more gradual WAM strengthening and vegetation shifts are predicted, but in some regional climate models the WAM instead collapses (87). Clearly, the existence of a future tipping threshold for the WAM and Sahel remains uncertain, as does its sign, but given multiple past abrupt shifts, known weaknesses in current models, huge regional impacts, but modest global climate feedback, we retain the Sahel/WAM as a potential regional impact tipping element [low confidence]. We adopt the scenario of abrupt wetting and greening with a threshold of ~2.8°C (2–3.5°C) [low confidence], timescale of 10y (10–50y) [low confidence], and uncertain Earth system impacts (regional warming) [medium confidence].

Low-latitude coral reefs (REEF). Tropical and subtropical coral reefs depend on a symbiotic association between coral and algae and on intense nutrient recycling (90). They are threatened by anthropogenic pressures including overfishing, direct damage, sedimentation (91), ocean acidification and global warming. When water temperatures exceed a certain threshold, coral irreversibly expel their symbiotic algae resulting in coral bleaching, thereby triggering coral death (92). Ocean acidification worsens warming-induced degradation. Coral collapse would remove one of the Earth’s most biodiverse ecosystems, impacting the wider marine food web, ocean nutrient and carbon cycling, and livelihoods for millions of people worldwide (91). Although coral bleaching is a localized process, synchronous bleaching can occur at ~1000km scale (as seen for the Great Barrier Reef), and further warming is expected to cause widespread bleaching (92). Adaptation may be possible with slower warming rates

(91), but the IPCC has projected 70-90% tropical/subtropical coral reef loss below 1.5°C, with near total loss by 2°C (88). Given regionally synchronized tipping dynamics with significant human but indirect climate impacts, we categorize warm-water coral reefs as a regional impact tipping element [high confidence]. Our best estimates are for a threshold of ~1.5°C (1-2°C) [high confidence], timescales of ~10y [medium confidence], and negligible GMST feedback [high confidence].

The **ocean biological pump** and **land/ocean carbon sink** are unlikely to be tipping elements, although they may feature nonlinearities (see SM).

Implications for climate policy and ‘safe’ levels of global warming

Fig. 2a summarizes our temperature threshold estimates for each tipping element making the shortlists (others are summarized in the Supplementary Text). Here we define crossing a CTP as ‘possible’ beyond its minimum temperature threshold and ‘likely’ beyond its best estimate.

[Fig. 2]

This revised assessment of CTPs has significant implications for climate policy, by determining ‘safe’ levels of global warming at which tipping either committed changes in Earth system function or major damages to future societies are avoided. Such a risk minimization approach, seeks to avoid minimum estimated thresholds for tipping elements, but this no longer appears possible for some.

Current warming is ~1.1°C above preindustrial, and even with rapid emission cuts warming will reach ~1.5°C by the 2030s (22). We cannot rule out that WAIS and GrIS tipping points have already been passed (see above) and several other tipping elements have minimum threshold values within the 1.1-1.5°C range. Our best estimate thresholds for GrIS, WAIS, warm-water corals (REEF) and abrupt permafrost thaw (PFAT) are ~1.5°C, although WAIS and GrIS collapse may still be avoidable if GMST returns below 1.5°C within an uncertain overshoot time (likely decades) (93). Setting aside achievability (and recognizing internal climate variability of $\sim\pm 0.1^\circ\text{C}$), this suggests ~1°C is a safe level of global

warming that minimizes the likelihood of crossing CTPs. This is consistent with the $<0.5-1^{\circ}\text{C}$ range of Holocene temperature variability, whereas past interglacials $\leq 1.5^{\circ}\text{C}$ had up to 10-13m higher sea level (20, 94).

The chance of triggering CTPs is already non-negligible, and will grow even with stringent climate mitigation (SSP1-1.9 in Fig. 2c). Nevertheless, achieving the Paris Agreement aim to “*strive to limit warming to 1.5°C* ” would clearly be safer than meeting the commitment to keep global warming below 2°C (88) (Fig. 2). Going from 1.5 to 2°C , the likelihood of committing to WAIS and GrIS collapse, near complete warm-water coral reef die-off, and abrupt permafrost thaw increases, and the best estimate threshold for LABC collapse is also crossed. The likelihood of triggering AMOC collapse, Boreal forest shifts, extra-polar glacier loss becomes non-negligible at $>1.5^{\circ}\text{C}$, and glacier loss becomes likely by $\sim 2^{\circ}\text{C}$. A cluster of abrupt shifts occur in ESM at $1.5-2^{\circ}\text{C}$ (18). While not tipping elements, ASSI loss could become regular by 2°C , gradual permafrost thaw would likely become widespread beyond 1.5°C , and land carbon sink weakening significant by 2°C .

Recent “Net Zero” targets if implemented could limit warming to $\sim 1.8^{\circ}\text{C}$ ($1.5-2.4^{\circ}\text{C}$) by 2100, but as of November 2021 existing pledges and targets would yield $\sim 2.1^{\circ}\text{C}$ ($1.7-2.6^{\circ}\text{C}$) or $\sim 2.4^{\circ}\text{C}$ ($1.9-3.0^{\circ}\text{C}$) for 2030 targets only, while current policies are estimated to result in $\sim 2.7^{\circ}\text{C}$ ($2.0-3.6^{\circ}\text{C}$) (95). $2-3^{\circ}\text{C}$ by 2100CE is therefore currently likely, with matching of pledges with policies key to determining where warming ends up in this range. Going from 2 to 3°C , maximum estimated thresholds for abrupt permafrost thaw, GrIS, WAIS, and extra-polar glaciers are passed, suggesting tipping them would become very likely. The likelihood of triggering EASB collapse, Amazon dieback, and West African monsoon shift (Sahel greening) becomes non-negligible at $\sim 2^{\circ}\text{C}$ and increases at $\sim 3^{\circ}\text{C}$. Sub-polar gyre collapse, boreal forest dieback and AMOC collapse also become more likely. While not tipping elements, above 2°C the Arctic would very likely become summer ice-free, and land carbon sink-to-source transitions would become widespread.

If the moderate ambition of current policies is not improved and climate sensitivity or carbon cycle feedbacks turn out to be higher than the median assumption then warming of up to $\sim 4^{\circ}\text{C}$ is possible by 2100CE, and $>4^{\circ}\text{C}$ cannot be ruled out if future policy ambition declines and/or implementation falters. Going from 3 to 5°C , EASB collapse becomes very likely, Amazon dieback becomes likely $>3.5^{\circ}\text{C}$, boreal forest shifts likely $>4^{\circ}\text{C}$, and large-scale permafrost collapse becomes possible at 3°C and likely $>4^{\circ}\text{C}$. AMOC collapse may become likely $>4^{\circ}\text{C}$ but with high uncertainty ($1.4\text{--}8^{\circ}\text{C}$ range), and Arctic winter sea ice collapse becomes possible $>4.5^{\circ}\text{C}$. Warming of $>5^{\circ}\text{C}$, whilst very unlikely this century, becomes plausible in the longer-term under higher climate sensitivities with current or reversed policies. This risks EAIS collapse and a commitment of $\sim 55\text{m}$ of sea level rise if warming stabilizes $>5^{\circ}\text{C}$ for multiple centuries. Other tipping elements if not already triggered – e.g. Amazon dieback, widespread Permafrost collapse – would very likely be committed, and AMOC collapse and Arctic winter sea ice collapse would become increasingly likely. Equatorial stratocumulus cloud breakup occurs in one model beyond $\sim 6^{\circ}\text{C}$ (96) and if plausible would represent a global CTP to a ‘Hothouse’ climate state (3).

Discussion

Tipping elements and their tipping points were treated independently in this assessment, but there are multiple causal interactions between them with risks of triggering cascades among CTPs (2, 4, 15), some mediated via temperature. The strength and in some cases even the sign of identified interactions is uncertain (4). Nevertheless, their combined effect tends to lower CTP temperature thresholds (6, 15). The present assessment would likely amplify this effect, further strengthening the incentive for ambitious mitigation.

Some of the threshold and impact estimates are highly uncertain (e.g. AMOC, BORF/TUND, AMAZ, SAHL, PFTP), and the transition timescale of many elements is uncertain. Some proposed elements remain too uncertain to categorize (e.g. EQSC, GOAE, INSM, AABW, Congo rainforest), and others considered unlikely to feature tipping dynamics (e.g. ENSO, JETI) cannot yet be fully ruled out (see SM).

Other tipping elements may yet be discovered. It may be possible to safely overshoot CTPs in slower elements like ice sheets (93), but the allowable overshoot times need further research. Spatial pattern formation might allow some biosphere elements to evade directly tipping (97), but this needs to be assessed.

To further our understanding of the likelihood of crossing CTPs, an updated expert elicitation (building on (4)) is overdue. A horizon-scanning exercise and systematic scanning of CMIP6 model output (following (18)) could help identify more candidate tipping elements. Further model improvements and model-data inter-comparison are essential. Early warning methods are starting to reveal whether tipping elements are destabilizing for parts of GrIS (11), AMOC (12), and the Amazon (98) and can reveal proximity to a CTP (11). They could be augmented with deep learning techniques (99). Systematic application to observational and remotely-sensed data, together with targeted new observing systems could begin to provide a CTP early warning system (100).

Conclusion

The UNFCCC stipulates that all countries commit to avoid "*dangerous climate change*", which through the Paris climate agreement translated into keeping GMST "*well below 2°C and aim for 1.5°C*". Our updated assessment of climate tipping elements and their tipping points suggests that "danger" may be approached even earlier. The Earth may have left a 'safe' climate state beyond 1°C global warming and above ~1.5°C global warming has significant likelihood of passing multiple climate tipping points, particularly in major ice sheets. Tipping point likelihood increases in the 'Paris range' of 1.5-2°C warming. This means that >1.5°C is not a 'safe' level of global warming. Current policies leading to ~2-3°C warming are 'unsafe' because they would likely trigger multiple climate tipping points. Our updated assessment of climate tipping points provides strong scientific support for the Paris Agreement and associated efforts to limit global warming to 1.5°C.

References and Notes:

1. T. M. Lenton, H. Held, E. Kriegler, J. W. Hall, W. Lucht, S. Rahmstorf, H. J. Schellnhuber, Tipping elements in the Earth's climate system. *Proc. Natl. Acad. Sci.* **105**, 1786–1793 (2008).
2. T. M. Lenton, J. Rockström, O. Gaffney, S. Rahmstorf, K. Richardson, W. Steffen, H. J. Schellnhuber, Climate tipping points — too risky to bet against. *Nature*. **575**, 592–595 (2019).
3. W. Steffen, J. Rockström, K. Richardson, T. M. Lenton, C. Folke, D. Liverman, C. P. Summerhayes, A. D. Barnosky, S. E. Cornell, M. Crucifix, J. F. Donges, I. Fetzer, S. J. Lade, M. Scheffer, R. Winkelmann, H. J. Schellnhuber, Trajectories of the Earth System in the Anthropocene. *Proc. Natl. Acad. Sci.* **115**, 8252–8259 (2018).
4. E. Kriegler, J. W. Hall, H. Held, R. Dawson, H. J. Schellnhuber, Imprecise probability assessment of tipping points in the climate system. *Proc. Natl. Acad. Sci.* **106**, 5041–5046 (2009).
5. H. J. Schellnhuber, S. Rahmstorf, R. Winkelmann, Why the right climate target was agreed in Paris. *Nat. Clim. Chang.* **6**, 649–653 (2016).
6. Y. Cai, T. M. Lenton, T. S. Lontzek, Risk of multiple interacting tipping points should encourage rapid CO₂ emission reduction. *Nat. Clim. Chang.* **6**, 1–5 (2016).
7. J. Feldmann, A. Levermann, Collapse of the West Antarctic Ice Sheet after local destabilization of the Amundsen Basin. *Proc. Natl. Acad. Sci.* **112**, 14191–14196 (2015).
8. M. S. Waibel, C. L. Hulbe, C. S. Jackson, D. F. Martin, Rate of Mass Loss Across the Instability Threshold for Thwaites Glacier Determines Rate of Mass Loss for Entire Basin. *Geophys. Res. Lett.* **45**, 809–816 (2018).
9. E. Rignot, J. Mouginot, M. Morlighem, H. Seroussi, B. Scheuchl, Widespread, rapid grounding line retreat of Pine Island, Thwaites, Smith, and Kohler glaciers, West Antarctica, from 1992 to

2011. *Geophys. Res. Lett.* **41**, 3502–3509 (2014).
10. I. Joughin, B. E. Smith, B. Medley, Marine Ice Sheet Collapse Potentially Under Way for the Thwaites Glacier Basin, West Antarctica. *Science*. **344**, 735–738 (2014).
11. N. Boers, M. Rypdal, Critical slowing down suggests that the western Greenland Ice Sheet is close to a tipping point. *Proc. Natl. Acad. Sci.* **118**, e2024192118 (2021).
12. N. Boers, Observation-based early-warning signals for a collapse of the Atlantic Meridional Overturning Circulation. *Nat. Clim. Chang.* **11**, 680–688 (2021).
13. W. Liu, S.-P. Xie, Z. Liu, J. Zhu, Overlooked possibility of a collapsed Atlantic Meridional Overturning Circulation in warming climate. *Sci. Adv.* **3**, e1601666 (2017).
14. W. Hubau, S. L. Lewis, O. L. Phillips, K. Affum-Baffoe, H. Beeckman, A. Cuní-Sanchez, A. K. Daniels, C. E. N. Ewango, S. Fauset, J. M. Mukinzi, D. Sheil, B. Sonké, M. J. P. Sullivan, T. C. H. Sunderland, H. Taedoumg, S. C. Thomas, L. J. T. White, K. A. Abernethy, S. Adu-Bredu, C. A. Amani, T. R. Baker, L. F. Banin, F. Baya, S. K. Begne, A. C. Bennett, F. Benedet, R. Bitariho, Y. E. Bocko, P. Boeckx, P. Boundja, R. J. W. Brienen, T. Brncic, E. Chezeaux, G. B. Chuyong, C. J. Clark, M. Collins, J. A. Comiskey, D. A. Coomes, G. C. Dargie, T. de Haulleville, M. N. D. Kamdem, J.-L. Doucet, A. Esquivel-Muelbert, T. R. Feldpausch, A. Fofanah, E. G. Foli, M. Gilpin, E. Gloor, C. Gonmadje, S. Gourlet-Fleury, J. S. Hall, A. C. Hamilton, D. J. Harris, T. B. Hart, M. B. N. Hockemba, A. Hladik, S. A. Ifo, K. J. Jeffery, T. Jucker, E. K. Yakusu, E. Kearsley, D. Kenfack, A. Koch, M. E. Leal, A. Levesley, J. A. Lindsell, J. Lisingo, G. Lopez-Gonzalez, J. C. Lovett, J.-R. Makana, Y. Malhi, A. R. Marshall, J. Martin, E. H. Martin, F. M. Mbayu, V. P. Medjibe, V. Mihindou, E. T. A. Mitchard, S. Moore, P. K. T. Munishi, N. N. Bengone, L. Ojo, F. E. Ondo, K. S.-H. Peh, G. C. Pickavance, A. D. Poulsen, J. R. Poulsen, L. Qie, J. Reitsma, F. Rovero, M. D. Swaine, J. Talbot, J. Taplin, D. M. Taylor, D. W. Thomas, B. Toirambe, J. T. Mukendi, D. Tuagben, P. M. Umunay, G. M. F. van der Heijden, H. Verbeeck, J.

- Vleminckx, S. Willcock, H. Wöll, J. T. Woods, L. Zemagho, Asynchronous carbon sink saturation in African and Amazonian tropical forests. *Nature*. **579**, 80–87 (2020).
15. N. Wunderling, J. F. Donges, J. Kurths, R. Winkelmann, Interacting tipping elements increase risk of climate domino effects under global warming. *Earth Syst. Dyn.* **12**, 601–619 (2021).
16. T. M. Lenton, Arctic Climate Tipping Points. *Ambio*. **41**, 10–22 (2012).
17. A. Staal, I. Fetzer, L. Wang-Erlandsson, J. H. C. Bosmans, S. C. Dekker, E. H. van Nes, J. Rockström, O. A. Tuinenburg, Hysteresis of tropical forests in the 21st century. *Nat. Commun.* **11**, 4978 (2020).
18. S. Drijfhout, S. Bathiany, C. Beaulieu, V. Brovkin, M. Claussen, C. Huntingford, M. Scheffer, G. Sgubin, D. Swingedouw, Catalogue of abrupt shifts in Intergovernmental Panel on Climate Change climate models. *Proc. Natl. Acad. Sci.* **112**, E5777–E5786 (2015).
19. A. Levermann, J. L. Bamber, S. Drijfhout, A. Ganopolski, W. Haeberli, N. R. P. Harris, M. Huss, K. Krüger, T. M. Lenton, R. W. Lindsay, D. Notz, P. Wadhams, S. Weber, Potential climatic transitions with profound impact on Europe. *Clim. Change*. **110**, 845–878 (2012).
20. B. Fox-Kemper, H. T. Hewitt, C. Xiao, G. Aðalgeirsdóttir, S. S. Drijfhout, T. L. Edwards, N. R. Golledge, M. Hemer, R. E. Kopp, G. Krinner, A. Mix, D. Notz, S. Nowicki, I. S. Nurhati, L. Ruiz, J.-B. Sallée, A. B. A. Slangen, Y. Yu, in *Climate Change 2021: The Physical Science Basis. Contribution of Working Group I to the Sixth Assessment Report of the Intergovernmental Panel on Climate Change*, V. Masson-Delmotte, P. Zhai, A. Pirani, S. L. Connors, C. Péan, S. Berger, N. Caud, Y. Chen, L. Goldfarb, M. I. Gomis, M. Huang, K. Leitzell, E. Lonnoy, J. B. R. Matthews, T. K. Maycock, T. Waterfield, O. Yelekçi, R. Yu, B. Zhou, Eds. (Cambridge University Press, 2021).
21. M. Collins, M. Sutherland, L. Bouwer, S.-M. Cheong, T. L. Frölicher, H. Jacot Des Combes, M. K. Roxy, I. Losada, K. L. McInnes, B. Ratter, E. Rivera-Arriaga, R. D. Susanto, D. Swingedouw,

- L. Tibig, P. Bakker, C. M. Eakin, K. Emanuel, M. Grose, M. Hemer, L. Jackson, A. Kääh, J. B. Kajtar, T. Knutson, C. Laufkötter, I. Noy, M. Payne, R. Ranasinghe, G. Sgubin, M.-L. Timmermans, in *IPCC Special Report on the Ocean and Cryosphere in a Changing Climate*, H.-O. Pörtner, D. C. Roberts, V. Masson-Delmotte, P. Zhai, M. Tignor, E. Poloczanska, K. Mintenbeck, A. Alegría, M. Nicolai, A. Okem, J. Petzold, B. Rama, N. M. Weyer, Eds. (2019; https://report.ipcc.ch/srocc/pdf/SROCC_FinalDraft_Chapter6.pdf), pp. 589–655.
22. J. Y. Lee, J. Marotzke, G. Bala, L. Cao, S. Corti, J. P. Dunne, F. Engelbrecht, E. Fischer, J. C. Fyfe, C. Jones, A. Maycock, J. Mutemi, O. Ndiaye, S. Panickal, T. Zhou, in *Climate Change 2021: The Physical Science Basis. Contribution of Working Group I to the Sixth Assessment Report of the Intergovernmental Panel on Climate Change*, V. Masson-Delmotte, P. Zhai, A. Pirani, S. L. Connors, C. Péan, S. Berger, N. Caud, Y. Chen, L. Goldfarb, M. I. Gomis, M. Huang, K. Leitzell, E. Lonnoy, J. B. R. Matthews, T. K. Maycock, T. Waterfield, O. Yelekçi, R. Yu, B. Zhou, Eds. (Cambridge University Press, 2021; <https://www.ipcc.ch/report/ar6/wg1/>).
 23. W. R. Boos, T. Storelvmo, Near-linear response of mean monsoon strength to a broad range of radiative forcings. *Proc. Natl. Acad. Sci. U. S. A.* **113**, 1510–1515 (2016).
 24. J. Garbe, T. Albrecht, A. Levermann, J. F. Donges, R. Winkelmann, The hysteresis of the Antarctic Ice Sheet. *Nature*. **585**, 538–544 (2020).
 25. R. Ranasinghe, A. C. Ruane, R. Vautard, N. Arnell, E. Coppola, F. A. Cruz, S. Dessai, A. S. Islam, M. Rahimi, D. R. Carrascal, J. Sillmann, M. B. Sylla, C. Tebaldi, W. Wang, R. Zaaboul, in *Climate Change 2021: The Physical Science Basis. Contribution of Working Group I to the Sixth Assessment Report of the Intergovernmental Panel on Climate Change*, V. Masson-Delmotte, P. Zhai, A. Pirani, S. L. Connors, C. Péan, S. Berger, N. Caud, Y. Chen, L. Goldfarb, M. I. Gomis, M. Huang, K. Leitzell, E. Lonnoy, J. B. R. Matthews, T. K. Maycock, T. Waterfield, O. Yelekçi,

- R. Yu, B. Zhou, Eds. (Cambridge University Press, 2021), p. 73.
26. National Research Council, *Abrupt Climate Change: Inevitable Surprises* (The National Academies Press, Washington, D.C., 2002; <http://www.nap.edu/catalog/10136>).
27. R. E. Kopp, R. L. Shwom, G. Wagner, J. Yuan, Tipping elements and climate–economic shocks: Pathways toward integrated assessment. *Earth's Futur.* **4**, 346–372 (2016).
28. M. Collins, R. Knutti, J. Arblaster, J.-L. Dufresne, T. Fichet, P. Friedlingstein, X. Gao, W. J. Gutowski, T. Johns, G. Krinner, M. Shongwe, C. Tebaldi, A. J. Weaver, M. Wehner, in *Climate Change 2013: The Physical Science Basis. Contribution of Working Group I to the Fifth Assessment Report of the Intergovernmental Panel on Climate Change*, T. F. Stocker, D. Qin, G.-K. Plattner, M. Tignor, S. K. Allen, J. Boschung, A. Nauels, Y. Xia, V. Bex, P. M. Midgley, Eds. (Cambridge University Press, Cambridge, UK; New York, USA, 2013; <https://www.ipcc.ch/report/ar5/wg1/long-term-climate-change-projections-commitments-and-irreversibility/>), pp. 1029–1136.
29. I. Allison, N. Bindoff, R. Bindshadler, *The Copenhagen Diagnosis* (2009; http://www.fcrn.org.uk/sites/default/files/Copenhagen_Diagnosis_2009.pdf).
30. D. Notz, S. Community, Arctic Sea Ice in CMIP6. *Geophys. Res. Lett.* **47**, 1–26 (2020).
31. C. Hankel, E. Tziperman, The Role of Atmospheric Feedbacks in Abrupt Winter Arctic Sea Ice Loss in Future Warming Scenarios. *J. Clim.* **34**, 4435–4447 (2021).
32. P. J. Hezel, T. Fichet, F. Massonnet, Modeled Arctic sea ice evolution through 2300 in CMIP5 extended RCPs. *Cryosph.* **8**, 1195–1204 (2014).
33. D. Docquier, R. Fuentes-Franco, T. Koenig, T. Fichet, Sea Ice—Ocean Interactions in the Barents Sea Modeled at Different Resolutions. *Front. Earth Sci.* **8**, 1–21 (2020).
34. F. Lehner, A. Born, C. C. Raible, T. F. Stocker, Amplified Inception of European Little Ice Age by

- Sea Ice–Ocean–Atmosphere Feedbacks. *J. Clim.* **26**, 7586–7602 (2013).
35. M. D. King, I. M. Howat, S. G. Candela, M. J. Noh, S. Jeong, B. P. Y. Noël, M. R. van den Broeke, B. Wouters, A. Negrete, Dynamic ice loss from the Greenland Ice Sheet driven by sustained glacier retreat. *Commun. Earth Environ.* **1**, 1–7 (2020).
 36. A. Shepherd, E. Ivins, E. Rignot, B. Smith, M. van den Broeke, I. Velicogna, P. Whitehouse, K. Briggs, I. Joughin, G. Krinner, S. Nowicki, T. Payne, T. Scambos, N. Schlegel, G. A. C. Agosta, A. Ahlstrøm, G. Babonis, V. R. Barletta, A. A. Bjørk, A. Blazquez, J. Bonin, W. Colgan, B. Csatho, R. Cullather, M. E. Engdahl, D. Felikson, X. Fettweis, R. Forsberg, A. E. Hogg, H. Gallee, A. Gardner, L. Gilbert, N. Gourmelen, A. Groh, B. Gunter, E. Hanna, C. Harig, V. Helm, A. Horvath, M. Horwath, S. Khan, K. K. Kjeldsen, H. Konrad, P. L. Langen, B. Lecavalier, B. Loomis, S. Luthcke, M. McMillan, D. Melini, S. Mernild, Y. Mohajerani, P. Moore, R. Mottram, J. Mouginot, G. Moyano, A. Muir, T. Nagler, G. Nield, J. Nilsson, B. Noël, I. Otosaka, M. E. Pattle, W. R. Peltier, N. Pie, R. Rietbroek, H. Rott, L. Sandberg Sørensen, I. Sasgen, H. Save, B. Scheuchl, E. Schrama, L. Schröder, K. W. Seo, S. B. Simonsen, T. Slater, G. Spada, T. Sutterley, M. Talpe, L. Tarasov, W. J. van de Berg, W. van der Wal, M. van Wessem, B. D. Vishwakarma, D. Wiese, D. Wilton, T. Wagner, B. Wouters, J. Wuite, Mass balance of the Greenland Ice Sheet from 1992 to 2018. *Nature*. **579**, 233–239 (2020).
 37. A. Robinson, R. Calov, A. Ganopolski, Multistability and critical thresholds of the Greenland ice sheet. *Nat. Clim. Chang.* **2**, 429–432 (2012).
 38. J. Van Breedam, H. Goelzer, P. Huybrechts, Semi-equilibrated global sea-level change projections for the next 10 000 years. *Earth Syst. Dyn.* **11**, 953–976 (2020).
 39. B. Noël, L. van Kampenhout, J. T. M. Lenaerts, W. J. van de Berg, M. R. van den Broeke, A 21st Century Warming Threshold for Sustained Greenland Ice Sheet Mass Loss. *Geophys. Res. Lett.* **48**, 1–9 (2021).

40. G. L. Foster, E. J. Rohling, Relationship between sea level and climate forcing by CO₂ on geological timescales. *Proc. Natl. Acad. Sci.* **110**, 1209–1214 (2013).
41. A. J. Christ, P. R. Bierman, J. M. Schaefer, D. Dahl-Jensen, J. P. Steffensen, L. B. Corbett, D. M. Peteet, E. K. Thomas, E. J. Steig, T. M. Rittenour, J.-L. Tison, P.-H. Blard, N. Perdrial, D. P. Dethier, A. Lini, A. J. Hidy, M. W. Caffee, J. Southon, A multimillion-year-old record of Greenland vegetation and glacial history preserved in sediment beneath 1.4 km of ice at Camp Century. *Proc. Natl. Acad. Sci.* **118**, e2021442118 (2021).
42. J. M. Gregory, S. E. George, R. S. Smith, Large and irreversible future decline of the Greenland ice sheet. *Cryosph.* **14**, 4299–4322 (2020).
43. R. B. Alley, S. Anandakrishnan, K. Christianson, H. J. Horgan, A. Muto, B. R. Parizek, D. Pollard, R. T. Walker, Oceanic Forcing of Ice-Sheet Retreat: West Antarctica and More. *Annu. Rev. Earth Planet. Sci.* **43**, 207–231 (2015).
44. C. S. M. Turney, C. J. Fogwill, N. R. Golledge, N. P. McKay, E. van Sebille, R. T. Jones, D. Etheridge, M. Rubino, D. P. Thornton, S. M. Davies, C. B. Ramsey, Z. A. Thomas, M. I. Bird, N. C. Munksgaard, M. Kohno, J. Woodward, K. Winter, L. S. Weyrich, C. M. Rootes, H. Millman, P. G. Albert, A. Rivera, T. van Ommen, M. Curran, A. Moy, S. Rahmstorf, K. Kawamura, C.-D. Hillenbrand, M. E. Weber, C. J. Manning, J. Young, A. Cooper, Early Last Interglacial ocean warming drove substantial ice mass loss from Antarctica. *Proc. Natl. Acad. Sci.* **117**, 3996–4006 (2020).
45. H. Yu, E. Rignot, H. Seroussi, M. Morlighem, Impact of iceberg calving on the retreat of Thwaites Glacier, West Antarctica over the next century with different calving laws and ocean thermal forcing, 1–13 (2019).
46. R. J. Arthern, C. R. Williams, The sensitivity of West Antarctica to the submarine melting feedback. *Geophys. Res. Lett.* **44**, 2352–2359 (2017).

47. T. L. Edwards, M. A. Brandon, G. Durand, N. R. Edwards, N. R. Golledge, P. B. Holden, I. J. Nias, A. J. Payne, C. Ritz, A. Wernecke, Revisiting Antarctic ice loss due to marine ice-cliff instability. *Nature*. **566**, 58–64 (2019).
48. R. M. DeConto, D. Pollard, R. B. Alley, I. Velicogna, E. Gasson, N. Gomez, S. Sadai, A. Condron, D. M. Gilford, E. L. Ashe, R. E. Kopp, D. Li, A. Dutton, The Paris Climate Agreement and future sea-level rise from Antarctica. *Nature*. **593**, 83–89 (2021).
49. D. J. Wilson, R. A. Bertram, E. F. Needham, T. van de Flierdt, K. J. Welsh, R. M. McKay, A. Mazumder, C. R. Riesselman, F. J. Jimenez-Espejo, C. Escutia, Ice loss from the East Antarctic Ice Sheet during late Pleistocene interglacials. *Nature*. **561**, 383–386 (2018).
50. P. U. Clark, F. He, N. R. Golledge, J. X. Mitrovica, A. Dutton, J. S. Hoffman, S. Dendy, Oceanic forcing of penultimate deglacial and last interglacial sea-level rise. *Nature*. **577**, 660–664 (2020).
51. E. Gasson, R. M. DeConto, D. Pollard, R. H. Levy, Dynamic Antarctic ice sheet during the early to mid-Miocene. *Proc. Natl. Acad. Sci.* **113**, 3459–3464 (2016).
52. E. A. G. Schuur, A. D. McGuire, C. Schädel, G. Grosse, J. W. Harden, D. J. Hayes, G. Hugelius, C. D. Koven, P. Kuhry, D. M. Lawrence, S. M. Natali, D. Olefeldt, V. E. Romanovsky, K. Schaefer, M. R. Turetsky, C. C. Treat, J. E. Vonk, Climate change and the permafrost carbon feedback. *Nature*. **520**, 171–179 (2015).
53. A. Vaks, O. S. Gutareva, S. F. M. Breitenbach, E. Avirmed, A. J. Mason, A. L. Thomas, A. V. Osinzev, A. M. Kononov, G. M. Henderson, Speleothems Reveal 500,000-Year History of Siberian Permafrost. *Science*. **340**, 183–186 (2013).
54. J. G. Josep G. Canadell, P. M. S. Monteiro, M. H. Costa, L. C. da Cunha, P. M. Cox, A. V. Eliseev, S. Henson, M. Ishii, S. Jaccard, C. Koven, A. Lohila, P. K. Patra, S. Piao, J. Rogelj, S. Syampungani, S. Zaehle, K. Zickfeld, in *Climate Change 2021: The Physical Science Basis*.

- Contribution of Working Group I to the Sixth Assessment Report of the Intergovernmental Panel on Climate Change 2021: The Physical Science Basis. Contribution of Working Group I to the Sixth Assessment Report*, V. Masson-Delmotte, P. Zhai, A. Pirani, S. L. Connors, C. Péan, S. Berger, N. Caud, Y. Chen, L. Goldfarb, M. I. Gomis, M. Huang, K. Leitzell, E. Lonnoy, J. B. R. Matthews, T. K. Maycock, T. Waterfield, O. Yelekçi, R. Yu, B. Zhou, Eds. (Cambridge University Press, 2021).
55. M. Turetsky, B. Abbott, M. Jones, K. M. Walter Anthony, D. Olefeldt, E. A. G. Schuur, G. Grosse, P. Kuhry, G. Hugelius, C. D. Koven, D. M. Lawrence, C. Gibson, A. Sannel, A. D. McGuire, Carbon release through abrupt permafrost thaw. *Nat. Geosci.* **13**, 138–143 (2020).
 56. B. Teufel, L. Sushama, Abrupt changes across the Arctic permafrost region endanger northern development. *Nat. Clim. Chang.* **9**, 858–862 (2019).
 57. J. Strauss, L. Schirrmeister, G. Grosse, D. Fortier, G. Hugelius, C. Knoblauch, V. Romanovsky, C. Schädel, T. Schneider von Deimling, E. A. G. Schuur, D. Shmelev, M. Ulrich, A. Veremeeva, Deep Yedoma permafrost: A synthesis of depositional characteristics and carbon vulnerability. *Earth-Science Rev.* **172**, 75–86 (2017).
 58. C. M. Luke, P. M. Cox, Soil carbon and climate change: from the Jenkinson effect to the compost-bomb instability. *Eur. J. Soil Sci.* **62**, 5–12 (2011).
 59. J. Hollesen, H. Matthiesen, A. B. Møller, B. Elberling, Permafrost thawing in organic Arctic soils accelerated by ground heat production. *Nat. Clim. Chang.* **5**, 574–578 (2015).
 60. M. Huss, R. Hock, Global-scale hydrological response to future glacier mass loss. *Nat. Clim. Chang.* **8**, 135–140 (2018).
 61. R. Hock, G. Rasul, C. Adler, B. Cáceres, S. Gruber, Y. Hirabayashi, M. Jackson, A. Kääb, S. Kang, S. Kutuzov, A. Milner, U. Molau, S. Morin, B. Orlove, H. I. Steltzer, in *IPCC Special*

- Report on the Ocean and Cryosphere in a Changing Climate*, H.-O. Pörtner, D. C. Roberts, V. Masson-Delmotte, P. Zhai, M. Tignor, E. Poloczanska, K. Mintenbeck, A. Alegría, M. Nicolai, A. Okem, J. Petzold, B. Rama, N. M. Weyer, Eds. (2019), pp. 131–202.
62. P. U. Clark, J. D. Shakun, S. A. Marcott, A. C. Mix, M. Eby, S. Kulp, A. Levermann, G. A. Milne, P. L. Pfister, B. D. Santer, D. P. Schrag, S. Solomon, T. F. Stocker, B. H. Strauss, A. J. Weaver, R. Winkelmann, D. Archer, E. Bard, A. Goldner, K. Lambeck, R. T. Pierrehumbert, G.-K. Plattner, Consequences of twenty-first-century policy for multi-millennial climate and sea-level change. *Nat. Clim. Chang.* **6**, 360–369 (2016).
 63. G. Sgubin, D. Swingedouw, S. Drijfhout, Y. Mary, A. Bennabi, Abrupt cooling over the North Atlantic in modern climate models. *Nat. Commun.* **8** (2017), doi:10.1038/ncomms14375.
 64. D. Swingedouw, A. Bily, C. Esquedo, L. F. Borchert, G. Sgubin, J. Mignot, M. Menary, On the risk of abrupt changes in the North Atlantic subpolar gyre in CMIP6 models. *Ann. N. Y. Acad. Sci.*, 1–15 (2021).
 65. J. Lynch-Stieglitz, The Atlantic Meridional Overturning Circulation and Abrupt Climate Change. *Ann. Rev. Mar. Sci.* **9**, 83–104 (2017).
 66. L. Caesar, S. Rahmstorf, A. Robinson, G. Feulner, V. Saba, Observed fingerprint of a weakening Atlantic Ocean overturning circulation. *Nature*. **556**, 191–196 (2018).
 67. J. Lohmann, P. D. Ditlevsen, Risk of tipping the overturning circulation due to increasing rates of ice melt. *Proc. Natl. Acad. Sci.* **118**, e2017989118 (2021).
 68. H. Douville, K. Raghavan, J. Renwick, R. P. Allan, P. A. Arias, M. Barlow, R. Cerezo-Mota, A. Cherchi, T. Y. Gan, J. Gergis, D. Jiang, A. Khan, W. P. Mba, D. Rosenfeld, J. Tierney, O. Zolina, in *Climate Change 2021: The Physical Science Basis. Contribution of Working Group I to the Sixth Assessment Report of the Intergovernmental Panel on Climate Change*, V. Masson-

- Delmotte, P. Zhai, A. Pirani, S. L. Connors, C. Péan, S. Berger, N. Caud, Y. Chen, L. Goldfarb, M. I. Gomis, M. Huang, K. Leitzell, E. Lonnoy, J. B. R. Matthews, T. K. Maycock, T. Waterfield, O. Yelekçi, R. Yu, B. Zhou, Eds. (Cambridge University Press, 2021), p. 73.
69. L. C. Jackson, R. Kahana, T. Graham, M. A. Ringer, T. Woollings, J. V. Mecking, R. A. Wood, Global and European climate impacts of a slowdown of the AMOC in a high resolution GCM. *Clim. Dyn.* **45**, 3299–3316 (2015).
70. S. Drijfhout, Competition between global warming and an abrupt collapse of the AMOC in Earth's energy imbalance. *Sci. Rep.* **5**, 14877 (2015).
71. A. Bozbiyik, M. Steinacher, F. Joos, T. F. Stocker, L. Menviel, Fingerprints of changes in the terrestrial carbon cycle in response to large reorganizations in ocean circulation. *Clim. Past.* **7**, 319–338 (2011).
72. L. V. Gatti, L. S. Basso, J. B. Miller, M. Gloor, L. G. Domingues, H. L. G. Cassol, G. Tejada, L. E. O. . Aragao, C. A. Nobre, W. Peter, L. Marani, E. Arai, A. H. Sanches, S. M. Correa, L. Anderson, C. von Randow, C. S. C. Correia, S. P. Crispim, R. A. L. Neves, Amazonia as a carbon source linked to deforestation and climate change. *Nature*. **595** (2021), doi:10.1038/s41586-021-03629-6.
73. Science Panel for the Amazon (SPA), “Executive Summary of the Amazon Assessment Report 2021” (2021), (available at <https://www.theamazonwewant.org/wp-content/uploads/2021/09/SPA-Executive-Summary-11Mb.pdf>).
74. A. Staal, O. A. Tuinenburg, J. H. C. Bosmans, M. Holmgren, E. H. Van Nes, M. Scheffer, D. C. Zemp, S. C. Dekker, Forest-rainfall cascades buffer against drought across the Amazon. *Nat. Clim. Chang.* **8**, 539–543 (2018).
75. D. C. Zemp, C.-F. Schleussner, H. M. J. Barbosa, M. Hirota, V. Montade, G. Sampaio, A. Staal, L.

- Wang-Erlandsson, A. Rammig, Self-amplified Amazon forest loss due to vegetation-atmosphere feedbacks. *Nat. Commun.* **8**, 14681 (2017).
76. C. A. Nobre, G. Sampaio, L. S. Borma, J. C. Castilla-Rubio, J. S. Silva, M. Cardoso, Land-use and climate change risks in the Amazon and the need of a novel sustainable development paradigm. *Proc. Natl. Acad. Sci.* **113**, 10759–10768 (2016).
 77. T. E. Lovejoy, C. Nobre, Amazon Tipping Point. *Sci. Adv.* **4**, eaat2340 (2018).
 78. P. M. Cox, D. Pearson, B. B. Booth, P. Friedlingstein, C. Huntingford, C. D. Jones, C. M. Luke, Sensitivity of tropical carbon to climate change constrained by carbon dioxide variability. *Nature.* **494**, 341–344 (2013).
 79. C. Terrer, R. B. Jackson, I. C. Prentice, T. F. Keenan, C. Kaiser, S. Vicca, J. B. Fisher, P. B. Reich, B. D. Stocker, B. A. Hungate, J. Peñuelas, I. McCallum, N. A. Soudzilovskaia, L. A. Cernusak, A. F. Talhelm, K. Van Sundert, S. Piao, P. C. D. Newton, M. J. Hovenden, D. M. Blumenthal, Y. Y. Liu, C. Müller, K. Winter, C. B. Field, W. Viechtbauer, C. J. Van Lissa, M. R. Hoosbeek, M. Watanabe, T. Koike, V. O. Leshyk, H. W. Polley, O. Franklin, Nitrogen and phosphorus constrain the CO₂ fertilization of global plant biomass. *Nat. Clim. Chang.* **9**, 684–689 (2019).
 80. M. Scheffer, M. Hirota, M. Holmgren, E. H. Van Nes, F. S. Chapin, Thresholds for boreal biome transitions. *Proc. Natl. Acad. Sci.* **109**, 21384–21389 (2012).
 81. B. Abis, V. Brovkin, Environmental conditions for alternative tree-cover states in high latitudes. *Biogeosciences.* **14**, 511–527 (2017).
 82. D. Gerten, W. Lucht, S. Ostberg, J. Heinke, M. Kowarsch, H. Kreft, Z. W. Kundzewicz, J. Rastgooy, R. Warren, H. J. Schellnhuber, Asynchronous exposure to global warming: freshwater resources and terrestrial ecosystems. *Environ. Res. Lett.* **8**, 034032 (2013).

83. C. D. Koven, Boreal carbon loss due to poleward shift in low-carbon ecosystems. *Nat. Geosci.* **6**, 452–456 (2013).
84. F. S. R. Pausata, M. Gaetani, G. Messori, A. Berg, D. Maia de Souza, R. F. Sage, P. B. deMenocal, The Greening of the Sahara: Past Changes and Future Implications. *One Earth.* **2**, 235–250 (2020).
85. M. W. Schmidt, P. Chang, A. O. Parker, L. Ji, F. He, Deglacial Tropical Atlantic subsurface warming links ocean circulation variability to the West African Monsoon. *Sci. Rep.* **7**, 1–11 (2017).
86. P. O. Hopcroft, P. J. Valdes, Paleoclimate-conditioning reveals a North Africa land–atmosphere tipping point. *Proc. Natl. Acad. Sci.* **118**, e2108783118 (2021).
87. A. Dosio, M. W. Jury, M. Almazroui, M. Ashfaq, I. Diallo, F. A. Engelbrecht, N. A. B. Klutse, C. Lennard, I. Pinto, M. B. Sylla, A. T. Tamoffo, Projected future daily characteristics of African precipitation based on global (CMIP5, CMIP6) and regional (CORDEX, CORDEX-CORE) climate models. *Clim. Dyn.* (2021), doi:10.1007/s00382-021-05859-w.
88. O. Hoegh-Guldberg, D. Jacob, M. Taylor, M. Bindi, S. Brown, I. Camilloni, A. Diedhiou, R. Djalante, K. L. Ebi, F. Engelbrecht, J. Guiot, Y. Hijikata, S. Mehrotra, A. Payne, S. I. Seneviratne, A. Thomas, R. Warren, G. Zhou, in *Global Warming of 1.5°C. An IPCC Special Report on the impacts of global warming of 1.5°C above pre-industrial levels and related global greenhouse gas emission pathways, in the context of strengthening the global response to the threat of climate change*, V. Masson-Delmotte, P. Zhai, H.-O. Pörtner, D. Roberts, J. Skea, P. R. Shukla, A. Pirani, W. Moufouma-Okia, C. Péan, R. Pidcock, S. Connors, J. B. R. Matthews, Y. Chen, X. Zhou, M. I. Gomis, E. Lonnoy, T. Maycock, M. Tignor, T. Waterfield, Eds. (2018), pp. 175–311.
89. A. Erfanian, G. Wang, M. Yu, R. Anyah, Multimodel ensemble simulations of present and future climates over West Africa: Impacts of vegetation dynamics. *J. Adv. Model. Earth Syst.* **8**, 1411–

1431 (2016).

90. J. M. De Goeij, D. Van Oevelen, M. J. A. Vermeij, R. Osinga, J. J. Middelburg, A. F. P. M. De Goeij, W. Admiraal, Surviving in a marine desert: The sponge loop retains resources within coral reefs. *Science*. **342**, 108–110 (2013).
91. T. P. Hughes, M. L. Barnes, D. R. Bellwood, J. E. Cinner, G. S. Cumming, J. B. C. Jackson, J. Kleypas, I. A. Van De Leemput, J. M. Lough, T. H. Morrison, S. R. Palumbi, E. H. Van Nes, M. Scheffer, Coral reefs in the Anthropocene. *Nature*. **546**, 82–90 (2017).
92. K. Frieler, M. Meinshausen, A. Golly, M. Mengel, K. Lebek, S. D. Donner, O. Hoegh-Guldberg, Limiting global warming to 2 °C is unlikely to save most coral reefs. *Nat. Clim. Chang.* **3**, 165–170 (2013).
93. P. D. L. Ritchie, J. J. Clarke, P. M. Cox, C. Huntingford, Overshooting tipping point thresholds in a changing climate. *Nature*. **592**, 517–523 (2021).
94. M. B. Osman, J. E. Tierney, J. Zhu, R. Tardif, G. J. Hakim, J. King, C. J. Poulsen, Globally resolved surface temperatures since the Last Glacial Maximum. *Nature*. **599**, 239–244 (2021).
95. Climate Analytics, NewClimate Institute, The Climate Action Tracker Thermometer (2021), (available at <https://climateactiontracker.org/global/cat-thermometer/>).
96. T. Schneider, C. M. Kaul, K. G. Pressel, Possible climate transitions from breakup of stratocumulus decks under greenhouse warming. *Nat. Geosci.* **12**, 164–168 (2019).
97. M. Rietkerk, R. Bastiaansen, S. Banerjee, J. Van De Koppel, Evasion of tipping in complex systems through spatial pattern formation. **169** (2021), doi:10.1126/science.abj0359.
98. C. A. Boulton, T. M. Lenton, B. N, Pronounced loss of Amazon rainforest resilience since the early 2000s. *Nat. Clim. Chang.*

99. T. M. Bury, R. I. Sujith, I. Pavithran, M. Scheffer, T. M. Lenton, M. Anand, C. T. Bauch, Deep learning for early warning signals of tipping points. *Proc. Natl. Acad. Sci.* **118**, e2106140118 (2021).
100. T. M. Lenton, Early warning of climate tipping points. *Nat. Clim. Chang.* **1**, 201–209 (2011).
101. A. Levermann, J. Schewe, V. Petoukhov, H. Held, Basic mechanism for abrupt monsoon transitions. *Proc. Natl. Acad. Sci. U. S. A.* **106**, 20572–20577 (2009).
102. K. Zickfeld, B. Knopf, V. Petoukhov, H. J. Schellnhuber, Is the Indian summer monsoon stable against global change? *Geophys. Res. Lett.* **32**, 1–5 (2005).
103. A. Levermann, V. Petoukhov, J. Schewe, H. J. Schellnhuber, Abrupt monsoon transitions as seen in paleorecords can be explained by moisture-advection feedback. *Proc. Natl. Acad. Sci. U. S. A.* **113**, e2348–e2349 (2016).
104. W. R. Boos, T. Storelvmo, Linear scaling for monsoons based on well-verified balance between adiabatic cooling and latent heat release. *Proc. Natl. Acad. Sci. U. S. A.* **113**, E2350–E2351 (2016).
105. A. Katzenberger, J. Schewe, J. Pongratz, A. Levermann, Robust increase of Indian monsoon rainfall and its variability under future warming in CMIP-6 models. *Earth Syst. Dyn. Discuss.*, 1–30 (2020).
106. A. J. Watson, T. M. Lenton, B. J. W. Mills, Ocean deoxygenation, the global phosphorus cycle and the possibility of human-caused large-scale ocean anoxia. *Philos. Trans. R. Soc. A Math. Phys. Eng. Sci.* **375**, 20160318 (2017).
107. H. C. Jenkyns, Geochemistry of oceanic anoxic events. *Geochemistry, Geophys. Geosystems.* **11**, 1–30 (2010).
108. T. P. Kemena, A. Landolfi, A. Oschlies, K. Wallmann, A. W. Dale, Ocean phosphorus inventory: large uncertainties in future projections on millennial timescales and their consequences for ocean

- deoxygenation. *Earth Syst. Dyn.* **10**, 539–553 (2019).
109. D. Niemeyer, T. P. Kemena, K. J. Meissner, A. Oschlies, A model study of warming-induced phosphorus-oxygen feedbacks in open-ocean oxygen minimum zones on millennial timescales. *Earth Syst. Dyn.* **8**, 357–367 (2017).
110. V. Lago, M. H. England, Projected Slowdown of Antarctic Bottom Water Formation in Response to Amplified Meltwater Contributions. *J. Clim.* **32**, 6319–6335 (2019).
111. J. Bjordal, T. Storelvmo, K. Alterskjær, T. Carlsen, Equilibrium climate sensitivity above 5 °C plausible due to state-dependent cloud feedback. *Nat. Geosci.* **13**, 718–721 (2020).
112. I. Tan, T. Storelvmo, M. D. Zelinka, Observational constraints on mixed-phase clouds imply higher climate sensitivity. *Science*. **352**, 224–227 (2016).
113. J. Zhu, C. J. Poulsen, On the Increase of Climate Sensitivity and Cloud Feedback With Warming in the Community Atmosphere Models. *Geophys. Res. Lett.* **47**, 1–10 (2020).
114. G. V. Cesana, A. D. Del Genio, Observational constraint on cloud feedbacks suggests moderate climate sensitivity. *Nat. Clim. Chang.* **11**, 213–218 (2021).
115. J. Zhu, C. J. Poulsen, B. L. Otto-Bliesner, High climate sensitivity in CMIP6 model not supported by paleoclimate. *Nat. Clim. Chang.* **10**, 378–379 (2020).
116. C. Senf, R. Seidl, Mapping the forest disturbance regimes of Europe. *Nat. Sustain.* **4**, 63–70 (2021).
117. S. Netherer, B. Panassiti, J. Pennerstorfer, B. Matthews, Acute Drought Is an Important Driver of Bark Beetle Infestation in Austrian Norway Spruce Stands. *Front. For. Glob. Chang.* **2**, 1–21 (2019).
118. G. Forzieri, M. Girardello, G. Ceccherini, J. Spinoni, L. Feyen, H. Hartmann, P. S. A. Beck, G.

- Camps-Valls, G. Chirici, A. Mauri, A. Cescatti, Emergent vulnerability to climate-driven disturbances in European forests. *Nat. Commun.* **12**, 1–12 (2021).
119. C. Senf, A. Buras, C. S. Zang, A. Rammig, R. Seidl, Excess forest mortality is consistently linked to drought across Europe. *Nat. Commun.* **11**, 1–8 (2020).
120. C. Senf, J. Sebold, R. Seidl, Increasing canopy mortality affects the future demographic structure of Europe's forests. *One Earth.* **4**, 749–755 (2021).
121. B. Schuldt, A. Buras, M. Arend, Y. Vitasse, C. Beierkuhnlein, A. Damm, M. Gharun, T. E. E. Grams, M. Hauck, P. Hajek, H. Hartmann, E. Hiltbrunner, G. Hoch, M. Holloway-Phillips, C. Körner, E. Larysch, T. Lübke, D. B. Nelson, A. Rammig, A. Rigling, L. Rose, N. K. Ruehr, K. Schumann, F. Weiser, C. Werner, T. Wohlgemuth, C. S. Zang, A. Kahmen, A first assessment of the impact of the extreme 2018 summer drought on Central European forests. *Basic Appl. Ecol.* **45**, 86–103 (2020).
122. A. Buras, A. Rammig, C. S. Zang, Quantifying impacts of the 2018 drought on European ecosystems in comparison to 2003. *Biogeosciences.* **17**, 1655–1672 (2020).
123. W. Peters, A. Bastos, P. Ciais, A. Vermeulen, A historical, geographical and ecological perspective on the 2018 European summer drought: Perspective on the 2018 European drought. *Philos. Trans. R. Soc. B Biol. Sci.* **375** (2020), doi:10.1098/rstb.2019.0505.
124. K. Albrich, W. Rammer, R. Seidl, Climate change causes critical transitions and irreversible alterations of mountain forests. *Glob. Chang. Biol.* **26**, 4013–4027 (2020).
125. E. M. Lansu, C. C. van Heerwaarden, A. I. Stegehuis, A. J. Teuling, Atmospheric Aridity and Apparent Soil Moisture Drought in European Forest During Heat Waves. *Geophys. Res. Lett.* **47** (2020), doi:10.1029/2020GL087091.
126. S. Wang, Y. Zhang, W. Ju, A. Porcar-Castell, S. Ye, Z. Zhang, C. Brümmer, M. Urbaniak, I.

- Mammarella, R. Juszczak, K. Folkert Boersma, Warmer spring alleviated the impacts of 2018 European summer heatwave and drought on vegetation photosynthesis. *Agric. For. Meteorol.* **295**, 108195 (2020).
127. A. J. Teuling, A hot future for European droughts. *Nat. Clim. Chang.* **8**, 364–365 (2018).
128. L. Samaniego, S. Thober, R. Kumar, N. Wanders, O. Rakovec, M. Pan, M. Zink, J. Sheffield, E. F. Wood, A. Marx, Anthropogenic warming exacerbates European soil moisture droughts. *Nat. Clim. Chang.* **8**, 421–426 (2018).
129. C. Gohr, J. S. Blumröder, D. Sheil, P. L. Ibisch, Quantifying the mitigation of temperature extremes by forests and wetlands in a temperate landscape. *Ecol. Inform.* **66** (2021), doi:10.1016/j.ecoinf.2021.101442.
130. G. Lasslop, V. Brovkin, C. H. Reick, S. Bathiany, S. Kloster, Multiple stable states of tree cover in a global land surface model due to a fire-vegetation feedback. *Geophys. Res. Lett.* **43**, 6324–6331 (2016).
131. D. T. Shindell, D. Rind, P. Lonergan, Increased polar stratospheric ozone losses and delayed eventual recovery owing to increasing greenhouse-gas concentrations. *Nature.* **392**, 589–592 (1998).
132. D. L. Hartmann, J. M. Wallace, V. Limpasuvan, D. W. J. Thompson, J. R. Holton, Can ozone depletion and global warming interact to produce rapid climate change? *Proc. Natl. Acad. Sci. U. S. A.* **97**, 1412–1417 (2000).
133. J. Austin, D. Shindell, S. R. Beagley, C. Brühl, M. Dameris, E. Manzini, T. Nagashima, P. Newman, S. Pawson, G. Pitari, E. Rozanov, C. Schnadt, T. G. Shepherd, Uncertainties and assessments of chemistry-climate models of the stratosphere. *Atmos. Chem. Phys.* **3**, 1–27 (2003).
134. B. Weatherhead, A. Tanskanen, A. Stevermer, S. B. Andersen, A. Arola, J. Austin, G. Bernhard,

- H. Browman, V. Fioletov, V. Grewe, J. Herman, W. Josefsson, A. Kylling, E. Kyrö, A. Lindfors, D. Shindell, P. Taalas, D. Tarasick, in *Arctic Climate Impact Assessment Report*, C. Symon, L. Arris, B. Heal, Eds. (Cambridge University Press, 2005; <http://www.acia.uaf.edu/pages/scientific.html>), pp. 151–182.
135. V. Eyring, N. P. Gillett, K. M. A. Rao, R. Barimalala, M. Barreiro Parrillo, N. Bellouin, C. Cassou, P. J. Durack, Y. Kosaka, S. McGregor, S. Min, O. Morgenstern, Y. Sun, in *Climate Change 2021: The Physical Science Basis. Contribution of Working Group I to the Sixth Assessment Report of the Intergovernmental Panel on Climate Change*, V. Masson-Delmotte, P. Zhai, A. Pirani, S. L. Connors, C. Péan, S. Berger, N. Caud, Y. Chen, L. Goldfarb, M. I. Gomis, M. Huang, K. Leitzell, E. Lonnoy, J. B. R. Matthews, T. K. Maycock, T. Waterfield, O. Yelekçi, R. Yu, B. Zhou, Eds. (Cambridge University Press, 2021; https://www.ipcc.ch/report/ar6/wg1/downloads/report/IPCC_AR6_WGI_Chapter_03.pdf).
136. J. A. Francis, S. J. Vavrus, Evidence for a wavier jet stream in response to rapid Arctic warming. *Environ. Res. Lett.* **10**, 014005 (2015).
137. R. Blackport, J. A. Screen, Weakened evidence for mid-latitude impacts of Arctic warming. *Nat. Clim. Chang.* **11**, 21–22 (2020).
138. F. J. Doblas-Reyes, A. A. Sörensson, M. Almazroui, A. Dosio, W. J. Gutowski, R. Haarsma, R. Hamdi, B. Hewitson, W.-T. Kwon, B. L. Lamptey, D. Maraun, T. S. Stephenson, I. Takayabu, L. Terray, A. Turner, Z. Zuo, in *Climate Change 2021: The Physical Science Basis. Contribution of Working Group I to the Sixth Assessment Report of the Intergovernmental Panel on Climate Change*, V. Masson-Delmotte, P. Zhai, A. Pirani, S. L. Connors, C. Péan, S. Berger, N. Caud, Y. Chen, L. Goldfarb, M. I. Gomis, M. Huang, K. Leitzell, E. Lonnoy, J. B. R. Matthews, T. K. Maycock, T. Waterfield, O. Yelekçi, R. Yu, B. Zhou, Eds. (Cambridge University Press, 2020).

139. K. Pistone, I. Eisenman, V. Ramanathan, Radiative Heating of an Ice-Free Arctic Ocean. *Geophys. Res. Lett.* **46**, 7474–7480 (2019).
140. D. Archer, B. Buffett, V. Brovkin, Ocean methane hydrates as a slow tipping point in the global carbon cycle. *Proc. Natl. Acad. Sci.* **106**, 20596–20601 (2009).
141. G. R. Dickens, Down the Rabbit Hole: toward appropriate discussion of methane release from gas hydrate systems during the Paleocene-Eocene thermal maximum and other past hyperthermal events. *Clim. Past.* **7**, 831–846 (2011).
142. G. R. Dickens, J. R. O. Neil, D. K. Rea, R. M. Owen, Dissociation of oceanic methane hydrate as a cause of the carbon isotope excursion at the end of the Paleocene. *Paleoceanography.* **10**, 965–971 (1995).
143. T. A. Minshull, H. Marín-Moreno, D. I. Armstrong McKay, P. A. Wilson, Mechanistic insights into a hydrate contribution to the Paleocene-Eocene carbon cycle perturbation from coupled thermohydraulic simulations. *Geophys. Res. Lett.* **43**, 8637–8644 (2016).
144. D. J. Lunt, A. Ridgwell, A. Sluijs, J. Zachos, S. Hunter, A. Haywood, A model for orbital pacing of methane hydrate destabilization during the Palaeogene. *Nat. Geosci.* **4**, 775–778 (2011).
145. D. I. Armstrong McKay, T. M. Lenton, Reduced carbon cycle resilience across the Palaeocene–Eocene Thermal Maximum. *Clim. Past.* **14**, 1515–1527 (2018).
146. J. C. Zachos, G. R. Dickens, R. E. Zeebe, An early Cenozoic perspective on greenhouse warming and carbon-cycle dynamics. *Nature.* **451**, 279–83 (2008).
147. S. Kender, K. Bogus, G. K. Pedersen, K. Dybkjær, T. A. Mather, E. Mariani, A. Ridgwell, J. B. Riding, T. Wagner, S. P. Hesselbo, M. J. Leng, Paleocene/Eocene carbon feedbacks triggered by volcanic activity. *Nat. Commun.* **12**, 5186 (2021).
148. M. Gutjahr, A. Ridgwell, P. F. Sexton, E. Anagnostou, P. N. Pearson, H. Pälike, R. D. Norris, E.

- Thomas, G. L. Foster, Very large release of mostly volcanic carbon during the Palaeocene–Eocene Thermal Maximum. *Nature*. **548**, 573–577 (2017).
149. H. Marín-Moreno, T. A. Minshull, G. K. Westbrook, B. Sinha, S. Sarkar, The response of methane hydrate beneath the seabed offshore Svalbard to ocean warming during the next three centuries. *Geophys. Res. Lett.* **40**, 5159–5163 (2013).
150. A. Vaks, A. J. Mason, S. F. M. Breitenbach, A. M. Kononov, A. V. Osinzev, M. Rosensaft, A. Borshevsky, O. S. Gutareva, G. M. Henderson, Palaeoclimate evidence of vulnerable permafrost during times of low sea ice. *Nature*. **577**, 221–225 (2020).
151. C. D. Koven, W. J. Riley, A. Stern, Analysis of Permafrost Thermal Dynamics and Response to Climate Change in the CMIP5 Earth System Models. *J. Clim.* **26**, 1877–1900 (2013).
152. M. Meinshausen, Z. R. J. Nicholls, J. Lewis, M. J. Gidden, E. Vogel, M. Freund, U. Beyerle, C. Gessner, A. Nauels, N. Bauer, J. G. Canadell, J. S. Daniel, A. John, P. B. Krummel, G. Luderer, N. Meinshausen, S. A. Montzka, P. J. Rayner, S. Reimann, S. J. Smith, M. van den Berg, G. J. M. Velders, M. K. Vollmer, R. H. J. Wang, The shared socio-economic pathway (SSP) greenhouse gas concentrations and their extensions to 2500. *Geosci. Model Dev.* **13**, 3571–3605 (2020).
153. A. H. MacDougall, C. A. Avis, A. J. Weaver, Significant contribution to climate warming from the permafrost carbon feedback. *Nat. Geosci.* **5**, 719–721 (2012).
154. E. J. Burke, C. D. Jones, C. D. Koven, Estimating the Permafrost-Carbon Climate Response in the CMIP5 Climate Models Using a Simplified Approach. *J. Clim.* **26**, 4897–4909 (2013).
155. T. Schneider von Deimling, G. Grosse, J. Strauss, L. Schirrmeister, A. Morgenstern, S. Schaphoff, M. Meinshausen, J. Boike, Observation-based modelling of permafrost carbon fluxes with accounting for deep carbon deposits and thermokarst activity. *Biogeosciences*. **12**, 3469–3488 (2015).

156. C. D. Koven, D. M. Lawrence, W. J. Riley, Permafrost carbon-climate feedback is sensitive to deep soil carbon decomposability but not deep soil nitrogen dynamics. *Proc. Natl. Acad. Sci. U. S. A.* **112**, 3752–3757 (2015).
157. K. Schaefer, H. Lantuit, V. E. Romanovsky, E. A. G. Schuur, R. Witt, The impact of the permafrost carbon feedback on global climate. *Environ. Res. Lett.* **9**, 085003 (2014).
158. M. R. Turetsky, B. W. Abbott, M. C. Jones, K. Walter Anthony, D. Olefeldt, E. A. G. Schuur, C. Koven, A. D. McGuire, G. Grosse, P. Kuhry, G. Hugelius, D. M. Lawrence, C. Gibson, A. B. K. Sannel, Permafrost collapse is accelerating carbon release. *Nature*. **569**, 32–34 (2019).
159. P. Friedlingstein, M. W. Jones, M. O’Sullivan, R. M. Andrew, J. Hauck, G. P. Peters, W. Peters, J. Pongratz, S. Sitch, C. Le Quéré, O. C. E. DBakker, J. G. Canadell, P. Ciais, R. B. Jackson, P. Anthoni, L. Barbero, A. Bastos, V. Bastrikov, M. Becker, L. Bopp, E. Buitenhuis, N. Chandra, F. Chevallier, L. P. Chini, K. I. Currie, R. A. Feely, M. Gehlen, D. Gilfillan, T. Gkritzalis, D. S. Goll, N. Gruber, S. Gutekunst, I. Harris, V. Haverd, R. A. Houghton, G. Hurtt, T. Ilyina, A. K. Jain, E. Joetzer, J. O. Kaplan, E. Kato, K. K. Goldewijk, J. I. Korsbakken, P. Landschützer, S. K. Lauvset, N. Lefèvre, A. Lenton, S. Lienert, D. Lombardozzi, G. Marland, P. C. McGuire, J. R. Melton, N. Metzl, D. R. Munro, J. E. M. S. Nabel, S. I. Nakaoka, C. Neill, A. M. Omar, T. Ono, A. Peregon, D. Pierrot, B. Poulter, G. Rehder, L. Resplandy, E. Robertson, C. Rödenbeck, R. Séférian, J. Schwinger, N. Smith, P. P. Tans, H. Tian, B. Tilbrook, F. N. Tubiello, G. R. Van Der Werf, A. J. Wiltshire, S. Zaehle, Global carbon budget 2019. *Earth Syst. Sci. Data*. **11**, 1783–1838 (2019).
160. W. S. Broecker, T.-H. Peng, *Tracers in the sea* (Lamont-Doherty Geological Observatory, Palisades, New York, 1982).
161. J. Segschneider, J. Bendtsen, Temperature-dependent remineralization in a warming ocean increases surface pCO₂ through changes in marine ecosystem composition. *Global Biogeochem. Cycles*. **27**, 1214–1225 (2013).

162. D. I. Armstrong McKay, S. E. Cornell, K. Richardson, J. Rockström, Resolving ecological feedbacks on the ocean carbon sink in Earth system models. *Earth Syst. Dyn.* **12**, 797–818 (2021).
163. C. Heinze, T. Blenckner, H. Martins, D. Rusiecka, R. Döscher, M. Gehlen, N. Gruber, E. Holland, Ø. Hov, F. Joos, J. B. R. Matthews, R. Rødven, S. Wilson, The quiet crossing of ocean tipping points. *Proc. Natl. Acad. Sci.* **118**, e2008478118 (2021).
164. D. H. Rothman, Thresholds of catastrophe in the Earth system. *Sci. Adv.* **3**, 1–13 (2017).
165. D. H. Rothman, Characteristic disruptions of an excitable carbon cycle. *Proc. Natl. Acad. Sci.* **116**, 14813–14822 (2019).
166. S. Wang, Y. Zhang, W. Ju, J. M. Chen, P. Ciais, A. Cescatti, J. Sardans, I. A. Janssens, M. Wu, J. A. Berry, E. Campbell, M. Fernández-Martínez, R. Alkama, S. Sitch, P. Friedlingstein, W. K. Smith, W. Yuan, W. He, D. Lombardozzi, M. Kautz, D. Zhu, S. Lienert, E. Kato, B. Poulter, T. G. M. Sanders, I. Krüger, R. Wang, N. Zeng, H. Tian, N. Vuichard, A. K. Jain, A. Wiltshire, V. Haverd, D. S. Goll, J. Peñuelas, Recent global decline of CO₂ fertilization effects on vegetation photosynthesis. *Science*. **370**, 1295–1300 (2020).
167. A. J. Winkler, R. B. Myneni, A. Hannart, S. Sitch, V. Haverd, D. Lombardozzi, V. K. Arora, J. Pongratz, J. E. M. S. Nabel, D. S. Goll, E. Kato, H. Tian, A. Arneth, P. Friedlingstein, A. K. Jain, S. Zaehle, V. Brovkin, Slowdown of the greening trend in natural vegetation with further rise in atmospheric CO₂. *Biogeosciences*. **18**, 4985–5010 (2021).
168. A. J. Winkler, R. B. Myneni, G. A. Alexandrov, V. Brovkin, Earth system models underestimate carbon fixation by plants in the high latitudes. *Nat. Commun.* **10** (2019), doi:10.1038/s41467-019-08633-z.
169. M. J. P. Sullivan, S. L. Lewis, K. Affum-Baffoe, C. Castilho, F. Costa, A. C. Sanchez, C. E. N.

Ewango, W. Hubau, B. Marimon, A. Monteagudo-Mendoza, L. Qie, B. Sonké, R. V. Martinez, T. R. Baker, R. J. W. Brienen, T. R. Feldpausch, D. Galbraith, M. Gloor, Y. Malhi, S. I. Aiba, M. N. Alexiades, E. C. Almeida, E. A. de Oliveira, E. Á. Dávila, P. A. Loayza, A. Andrade, S. A. Vieira, L. E. O. C. Aragão, A. Araujo-Murakami, E. J. M. M. Arets, L. Arroyo, P. Ashton, G. Aymard C, F. B. Baccaro, L. F. Banin, C. Baraloto, P. B. Camargo, J. Barlow, J. Barroso, J. F. Bastin, S. A. Batterman, H. Beeckman, S. K. Begne, A. C. Bennett, E. Berenguer, N. Berry, L. Blanc, P. Boeckx, J. Bogaert, D. Bonal, F. Bongers, M. Bradford, F. Q. Brearley, T. Brncic, F. Brown, B. Burban, J. L. Camargo, W. Castro, C. Céron, S. C. Ribeiro, V. C. Moscoso, J. Chave, E. Chezeaux, C. J. Clark, F. C. de Souza, M. Collins, J. A. Comiskey, F. C. Valverde, M. C. Medina, L. da Costa, M. Dančák, G. C. Dargie, S. Davies, N. D. Cardozo, T. de Haulleville, M. B. de Medeiros, J. Del Aguila Pasquel, G. Derroire, A. Di Fiore, J. L. Doucet, A. Dourdain, V. Droissart, L. F. Duque, R. Ekoungoulou, F. Elias, T. Erwin, A. Esquivel-Muelbert, S. Fauset, J. Ferreira, G. F. Llampazo, E. Foli, A. Ford, M. Gilpin, J. S. Hall, K. C. Hamer, A. C. Hamilton, D. J. Harris, T. B. Hart, R. Hédli, B. Herault, R. Herrera, N. Higuchi, A. Hladik, E. H. Coronado, I. Huamantupa-Chuquimaco, W. H. Huasco, K. J. Jeffery, E. Jimenez-Rojas, M. Kalamandeen, M. N. K. Djuikouo, E. Kearsley, R. K. Umetsu, L. K. Kho, T. Killeen, K. Kitayama, B. Klitgaard, A. Koch, N. Labrière, W. Laurance, S. Laurance, M. E. Leal, A. Levesley, A. J. N. Lima, J. Lisingo, A. P. Lopes, G. Lopez-Gonzalez, T. Lovejoy, J. C. Lovett, R. Lowe, W. E. Magnusson, J. Malumbres-Olarte, Â. G. Manzatto, B. H. Marimon, A. R. Marshall, T. Marthews, S. M. de Almeida Reis, C. Maycock, K. Melgaço, C. Mendoza, F. Metali, V. Mihindou, W. Milliken, E. T. A. Mitchard, P. S. Morandi, H. L. Mossman, L. Nagy, H. Nascimento, D. Neill, R. Nilus, P. N. Vargas, W. Palacios, N. P. Camacho, J. Peacock, C. Pendry, M. C. Peñuela Mora, G. C. Pickavance, J. Pipoly, N. Pitman, M. Playfair, L. Poorter, J. R. Poulsen, A. D. Poulsen, R. Preziosi, A. Prieto, R. B. Primack, H. Ramírez-Angulo, J. Reitsma, M. Réjou-Méchain, Z. R. Correa, T. R. de Sousa, L. R. Bayona, A. Roopsind, A. Rudas, E. Rutishauser, K. Abu Salim, R. P. Salomão, J. Schietti, D. Sheil, R. C. Silva, J. S. Espejo, C. S. Valeria, M. Silveira, M. Simo-

- Droissart, M. F. Simon, J. Singh, Y. C. Soto Shareva, C. Stahl, J. Stropp, R. Sukri, T. Sunderland, M. Svátek, M. D. Swaine, V. Swamy, H. Taedoumg, J. Talbot, J. Taplin, D. Taylor, H. Ter Steege, J. Terborgh, R. Thomas, S. C. Thomas, A. Torres-Lezama, P. Umunay, L. V. Gamarra, G. van der Heijden, P. van der Hout, P. van der Meer, M. van Nieuwstadt, H. Verbeeck, R. Vernimmen, A. Vicentini, I. C. G. Vieira, E. V. Torre, J. Vleminckx, V. Vos, O. Wang, L. J. T. White, S. Willcock, J. T. Woods, V. Wortel, K. Young, R. Zagt, L. Zemagho, P. A. Zuidema, J. A. Zwerts, O. L. Phillips, Long-term thermal sensitivity of Earth's tropical forests. *Science*. **368**, 869–874 (2020).
170. R. J. W. Brienen, O. L. Phillips, T. R. Feldpausch, E. Gloor, T. R. Baker, J. Lloyd, G. Lopez-Gonzalez, A. Monteagudo-Mendoza, Y. Malhi, S. L. Lewis, R. Vásquez Martinez, M. Alexiades, E. Álvarez Dávila, P. Alvarez-Loayza, A. Andrade, L. E. O. C. Aragaõ, A. Araujo-Murakami, E. J. M. M. Arets, L. Arroyo, G. A. Aymard C., O. S. Bánki, C. Baraloto, J. Barroso, D. Bonal, R. G. A. Boot, J. L. C. Camargo, C. V. Castilho, V. Chama, K. J. Chao, J. Chave, J. A. Comiskey, F. Cornejo Valverde, L. Da Costa, E. A. De Oliveira, A. Di Fiore, T. L. Erwin, S. Fauset, M. Forsthofer, D. R. Galbraith, E. S. Grahame, N. Groot, B. Hérault, N. Higuchi, E. N. Honorio Coronado, H. Keeling, T. J. Killeen, W. F. Laurance, S. Laurance, J. Licona, W. E. Magnussen, B. S. Marimon, B. H. Marimon-Junior, C. Mendoza, D. A. Neill, E. M. Nogueira, P. Núñez, N. C. Pallqui Camacho, A. Parada, G. Pardo-Molina, J. Peacock, M. Penã-Claros, G. C. Pickavance, N. C. A. Pitman, L. Poorter, A. Prieto, C. A. Quesada, F. Ramírez, H. Ramírez-Angulo, Z. Restrepo, A. Roopsind, A. Rudas, R. P. Salomaõ, M. Schwarz, N. Silva, J. E. Silva-Espejo, M. Silveira, J. Stropp, J. Talbot, H. Ter Steege, J. Teran-Aguilar, J. Terborgh, R. Thomas-Caesar, M. Toledo, M. Torello-Raventos, R. K. Umetsu, G. M. F. Van Der Heijden, P. Van Der Hout, I. C. Guimarães Vieira, S. A. Vieira, E. Vilanova, V. A. Vos, R. J. Zagt, Long-term decline of the Amazon carbon sink. *Nature*. **519**, 344–348 (2015).
171. L. V. Gatti, L. S. Basso, J. B. Miller, M. Gloor, L. Gatti Domingues, H. L. G. Cassol, G. Tejada,

- L. E. O. C. Aragão, C. Nobre, W. Peters, L. Marani, E. Arai, A. H. Sanches, S. M. Corrêa, L. Anderson, C. Von Randow, C. S. C. Correia, S. P. Crispim, R. A. L. Neves, Amazonia as a carbon source linked to deforestation and climate change. *Nature*. **595**, 388–393 (2021).
172. T. Tagesson, G. Schurgers, S. Horion, P. Ciais, F. Tian, M. Brandt, A. Ahlström, J. P. Wigner, J. Ardö, S. Olin, L. Fan, Z. Wu, R. Fensholt, Recent divergence in the contributions of tropical and boreal forests to the terrestrial carbon sink. *Nat. Ecol. Evol.* **4**, 202–209 (2020).
173. K. A. Duffy, C. R. Schwalm, V. L. Arcus, G. W. Koch, L. L. Liang, L. A. Schipper, How close are we to the temperature tipping point of the terrestrial biosphere? *Sci. Adv.* **7**, eaay1052 (2021).
174. P. Zhang, J. H. Jeong, J. H. Yoon, H. Kim, S. Y. Simon Wang, H. W. Linderholm, K. Fang, X. Wu, D. Chen, Abrupt shift to hotter and drier climate over inner East Asia beyond the tipping point. *Science*. **370**, 1095–1099 (2020).
175. Y. van der Velde, A. J. A. M. Temme, J. J. Nijp, M. C. Braakhekke, G. A. K. van Voorn, S. C. Dekker, A. J. Dolman, J. Wallinga, K. J. Devito, N. Kettridge, C. A. Mendoza, L. Kooistra, M. B. Soons, A. J. Teuling, Emerging forest–peatland bistability and resilience of European peatland carbon stores. *Proc. Natl. Acad. Sci.* **118**, e2101742118 (2021).
176. R. M. Varney, S. E. Chadburn, P. Friedlingstein, E. J. Burke, C. D. Koven, G. Hugelius, P. M. Cox, A spatial emergent constraint on the sensitivity of soil carbon turnover to global warming. *Nat. Commun.* **11**, 5544 (2020).
177. S. S. Saatchi, N. L. Harris, S. Brown, M. Lefsky, E. T. A. Mitchard, W. Salas, B. R. Zutta, W. Buermann, S. L. Lewis, S. Hagen, S. Petrova, L. White, M. Silman, A. Morel, Benchmark map of forest carbon stocks in tropical regions across three continents. *Proc. Natl. Acad. Sci. U. S. A.* **108**, 9899–9904 (2011).
178. E. M. Nogueira, A. M. Yanai, F. O. R. Fonseca, P. M. Fearnside, Carbon stock loss from

- deforestation through 2013 in Brazilian Amazonia. *Glob. Chang. Biol.* **21**, 1271–1292 (2015).
179. V. H. A. Heinrich, R. Dalagnol, H. L. G. Cassol, T. M. Rosan, C. T. de Almeida, C. H. L. Silva Junior, W. A. Campanharo, J. I. House, S. Sitch, T. C. Hales, M. Adami, L. O. Anderson, L. E. O. C. Aragão, Large carbon sink potential of secondary forests in the Brazilian Amazon to mitigate climate change. *Nat. Commun.* **12**, 1785 (2021).
180. B. Zimbres, P. Rodríguez-Veiga, J. Z. Shimbo, P. da Conceição Bispo, H. Balzter, M. Bustamante, I. Roitman, R. Haidar, S. Miranda, L. Gomes, F. Alvim Carvalho, E. Lenza, L. Maracahipes-Santos, A. C. Abadia, J. A. do Prado Júnior, E. L. Mendonça Machado, A. P. Dias Gonzaga, M. de Castro Nunes Santos Terra, J. M. de Mello, J. R. Soares Scolforo, J. R. Rodrigues Pinto, A. Alencar, Mapping the stock and spatial distribution of aboveground woody biomass in the native vegetation of the Brazilian Cerrado biome. *For. Ecol. Manage.* **499** (2021), doi:10.1016/j.foreco.2021.119615.
181. P. S. Morandi, B. S. Marimon, B. H. Marimon-Junior, J. A. Ratter, T. R. Feldpausch, G. R. Colli, C. B. R. Munhoz, M. C. da Silva Júnior, E. de Souza Lima, R. F. Haidar, L. Arroyo, A. A. Murakami, F. de Góis Aquino, B. M. T. Walter, J. F. Ribeiro, R. Françoso, F. Elias, E. A. de Oliveira, S. M. Reis, B. de Oliveira, E. C. das Neves, D. S. Nogueira, H. S. Lima, T. P. de Carvalho, S. A. Rodrigues, D. Villarroel, J. M. Felfili, O. L. Phillips, Tree diversity and above-ground biomass in the South America Cerrado biome and their conservation implications. *Biodivers. Conserv.* **29**, 1519–1536 (2020).
182. H. S. Barros, P. M. Fearnside, Soil carbon stock changes due to edge effects in central Amazon forest fragments. *For. Ecol. Manage.* **379**, 30–36 (2016).
183. S. Bathiany, M. Claussen, V. Brovkin, T. Raddatz, V. Gayler, Combined biogeophysical and biogeochemical effects of large-scale forest cover changes in the MPI earth system model. *Biogeosciences.* **7**, 1383–1399 (2010).

184. M. Hirota, M. Holmgren, E. H. Van Nes, M. Scheffer, Global Resilience of Tropical Forest and Savanna to Critical Transitions. *Science*. **334**, 232–235 (2011).
185. A. C. Staver, S. Archibald, S. A. Levin, The Global Extent and Determinants of Savanna and Forest as Alternative Biome States. *Science*. **334**, 230–232 (2011).
186. Y. Pan, R. A. Birdsey, J. Fang, R. Houghton, P. E. Kauppi, W. A. Kurz, O. L. Phillips, A. Shvidenko, S. L. Lewis, J. G. Canadell, P. Ciais, R. B. Jackson, S. W. Pacala, A. D. McGuire, S. Piao, A. Rautiainen, S. Sitch, D. Hayes, A Large and Persistent Carbon Sink in the World's Forests. *Science*. **333**, 988–993 (2011).
187. C. J. A. Bradshaw, I. G. Warkentin, Global estimates of boreal forest carbon stocks and flux. *Glob. Planet. Change*. **128**, 24–30 (2015).
188. M. Thurner, C. Beer, M. Santoro, N. Carvalhais, T. Wutzler, D. Schepaschenko, A. Shvidenko, E. Kompter, B. Ahrens, S. R. Levick, C. Schmullius, Carbon stock and density of northern boreal and temperate forests. *Glob. Ecol. Biogeogr.* **23**, 297–310 (2014).
189. O. A. Carpino, A. A. Berg, W. L. Quinton, J. R. Adams, Climate change and permafrost thaw-induced boreal forest loss in northwestern Canada. *Environ. Res. Lett.* **13** (2018), doi:10.1088/1748-9326/aad74e.
190. K. D. Dearborn, C. A. Wallace, R. Patankar, J. L. Baltzer, Permafrost thaw in boreal peatlands is rapidly altering forest community composition. *J. Ecol.* **109**, 1452–1467 (2021).
191. G. Grosse, S. Goetz, A. D. McGuire, V. E. Romanovsky, E. A. G. Schuur, Changing permafrost in a warming world and feedbacks to the Earth system. *Environ. Res. Lett.* **11**, 040201 (2016).
192. M. Williams, Y. Zhang, C. Estop-Aragonés, J. P. Fisher, G. Xenakis, D. J. Charman, I. P. Hartley, J. B. Murton, G. K. Phoenix, Boreal permafrost thaw amplified by fire disturbance and precipitation increases. *Environ. Res. Lett.* **15** (2020), doi:10.1088/1748-9326/abbeb8.

193. C. M. Gibson, L. E. Chasmer, D. K. Thompson, W. L. Quinton, M. D. Flannigan, D. Olefeldt, Wildfire as a major driver of recent permafrost thaw in boreal peatlands. *Nat. Commun.* **9** (2018), doi:10.1038/s41467-018-05457-1.
194. P. de Vrese, T. Stacke, T. Kleinen, V. Brovkin, Diverging responses of high-latitude CO₂ and CH₄ emissions in idealized climate change scenarios. *Cryosph.* **15**, 1097–1130 (2021).
195. A. D. McGuire, D. M. Lawrence, C. Koven, J. S. Clein, E. Burke, G. Chen, E. Jafarov, A. H. MacDougall, S. Marchenko, D. Nicolsky, S. Peng, A. Rinke, P. Ciais, I. Gouttevin, D. J. Hayes, D. Ji, G. Krinner, J. C. Moore, V. Romanovsky, C. Schädel, K. Schaefer, E. A. G. Schuur, Q. Zhuang, Dependence of the evolution of carbon dynamics in the northern permafrost region on the trajectory of climate change. *Proc. Natl. Acad. Sci. U. S. A.* **115**, 3882–3887 (2018).
196. C. D. Koven, E. A. G. Schuur, C. Schädel, T. J. Bohn, E. J. Burke, G. Chen, X. Chen, P. Ciais, G. Grosse, J. W. Harden, D. J. Hayes, G. Hugelius, E. E. Jafarov, G. Krinner, P. Kuhry, D. M. Lawrence, A. H. MacDougall, S. S. Marchenko, A. D. McGuire, S. M. Natali, D. J. Nicolsky, D. Olefeldt, S. Peng, V. E. Romanovsky, K. M. Schaefer, J. Strauss, C. C. Treat, M. Turetsky, A simplified, data-constrained approach to estimate the permafrost carbon–climate feedback. *Philos. Trans. R. Soc. A Math. Phys. Eng. Sci.* **373**, 20140423 (2015).
197. J. Obu, S. Westermann, A. Bartsch, N. Berdnikov, H. H. Christiansen, A. Dashtseren, R. Delaloye, B. Elberling, B. Etzelmüller, A. Kholodov, A. Khomutov, A. Kääb, M. O. Leibman, A. G. Lewkowicz, S. K. Panda, V. Romanovsky, R. G. Way, A. Westergaard-Nielsen, T. Wu, J. Yamkhin, D. Zou, Northern Hemisphere permafrost map based on TTOP modelling for 2000–2016 at 1 km² scale. *Earth-Science Rev.* **193**, 299–316 (2019).
198. FAO, ITPS, *Recarbonizing global soils – A technical manual of recommended management practices* (FAO, Rome, 2021; <http://www.fao.org/documents/card/en/c/cb6378en>), vol. 4.
199. C. Schädel, E. A. G. Schuur, R. Bracho, B. Elberling, C. Knoblauch, H. Lee, Y. Luo, G. R.

- Shaver, M. R. Turetsky, Circumpolar assessment of permafrost C quality and its vulnerability over time using long-term incubation data. *Glob. Chang. Biol.* **20**, 641–652 (2014).
200. B. Elberling, A. Michelsen, C. Schädel, E. A. G. Schuur, H. H. Christiansen, L. Berg, M. P. Tamstorf, C. Sigsgaard, Long-term CO₂ production following permafrost thaw. *Nat. Clim. Chang.* **3**, 890–894 (2013).

Acknowledgements:

Funding:

This work was initiated and supported by the European Research Council Advanced Investigator project “Earth Resilience in the Anthropocene” ERC-2016-ADG-743080 (DIAM, AS, SC, IF, JR)

The Earth Commission (supported by the Global Challenges Foundation and the Global Commons Alliance, a sponsored project of Rockefeller Philanthropy Advisors with support from Oak Foundation, MAVA, Porticus, Gordon and Betty Moore Foundation, Herlin Foundation and the Global Environment Facility) (DIAM, JFA, RW, BS, SL, JR)

Leverhulme Trust RPG-2018-046 (TML)

Turing Fellowship (TML)

Author contributions:

Conceptualization: DIAM, AS, IF, SEC, TML

Methodology & Investigation: DIAM

Visualization: JFA, BS, SL

Funding acquisition: JR

Writing – original draft: DIAM, TML

Writing – review & editing: DIAM, AS, JFA, RW, BS, SL, IF, SEC, JR, TML

Competing interests: The authors declare no competing financial interests.

Data and materials availability: All data is available in the manuscript or the supplementary materials.

Figures and Tables:

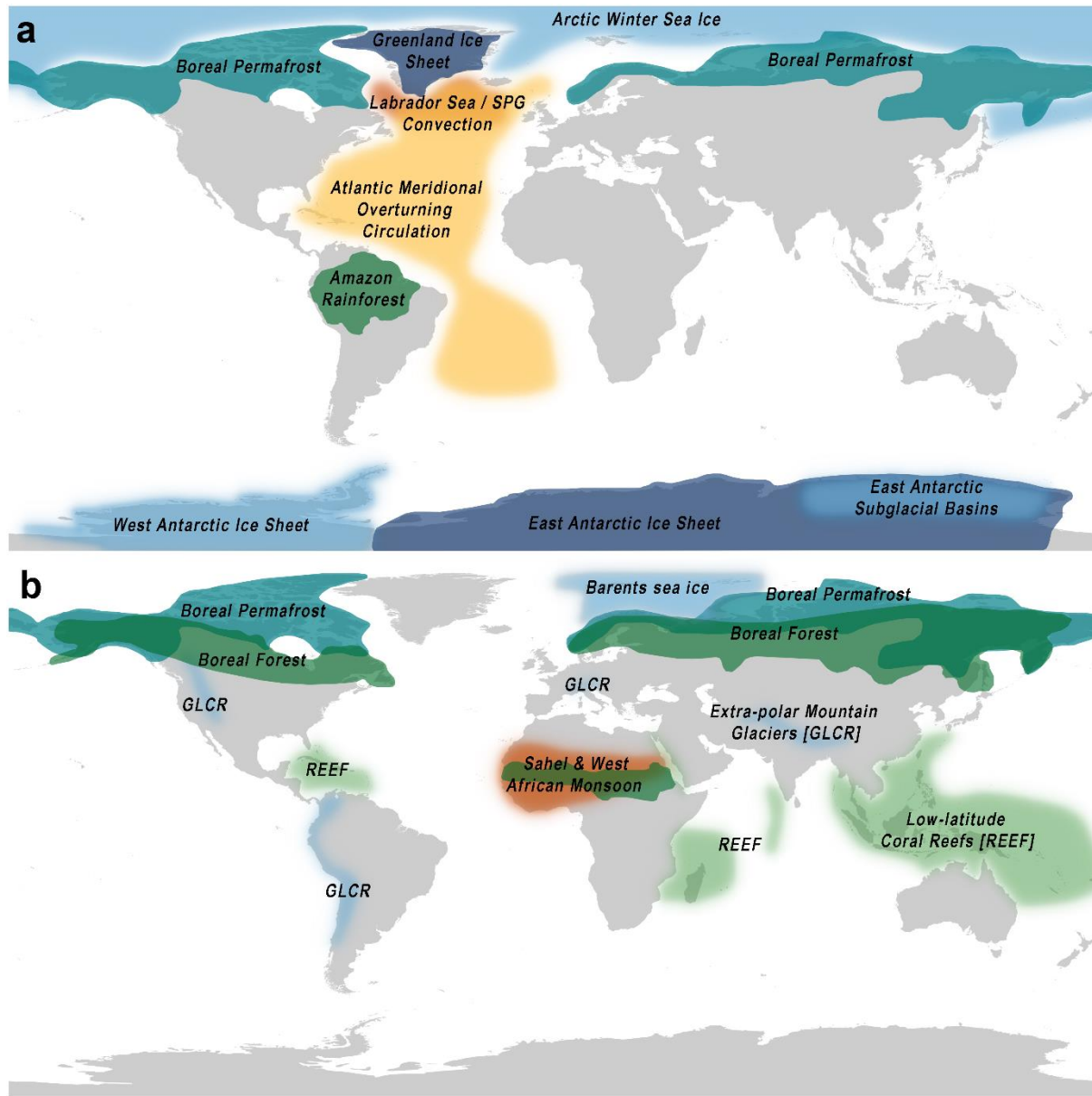


Fig. 1. Maps showing the global ‘core’ (a) and regional ‘impact’ (b) climate tipping elements identified in this study. Blue areas represent cryosphere elements, green biosphere, and orange ocean-atmosphere.

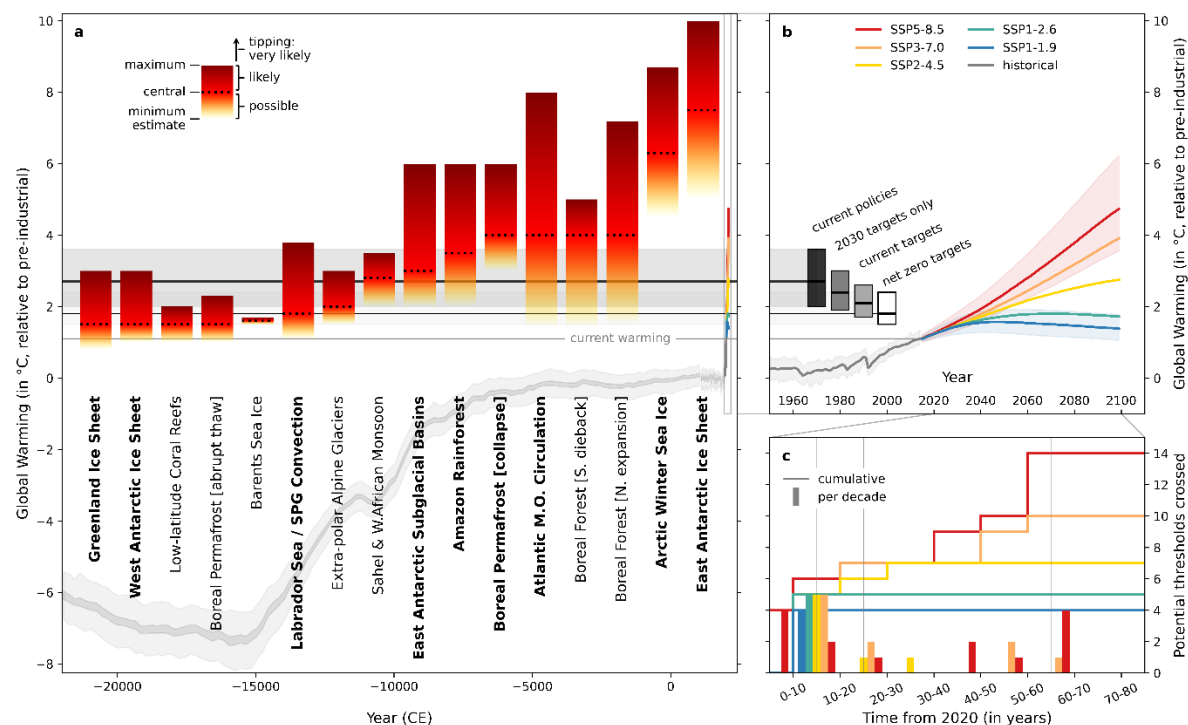


Fig. 2. Our global warming threshold estimates for global ‘core’ and regional ‘impact’ climate tipping elements (a) relative to IPCC SSP projections and likely future scenarios given current policies and targets (b) and how many thresholds may be crossed per SSP projection (c). Bars in (a) show the minimum (base, yellow), central (line, red), and maximum (top, dark red) threshold estimates, with a palaeorecord of GMST over the past ~25Ky (94) and projections of future climate change (green, SSP1-1.9; yellow, SSP1-2.6; orange, SSP2-4.5; red, SSP3-7.0; purple, SSP5-8.5) from IPCC AR6 (22) shown for context. Future projections are shown in more detail in (b), along with estimated 21st century warming trajectories from Climate Action Tracker (grey bars, extending into (a)); horizontal lines show central estimates, bar height the uncertainty ranges) as of November 2021 (95). The number of thresholds potentially passed in the coming decades depending on SSP trajectory in (c) is shown per decade (bars) and cumulatively (lines).

Table 1. Table showing our literature-based threshold, timescale, and impact estimates for the tipping elements we categorize as global ‘core’ or regional ‘impact’. Element acronym colors indicate Earth system domain (blue, cryosphere; green, biosphere; orange, ocean-atmosphere), and element name and estimate colors indicate subjective confidence levels (green, high; yellow, medium; red, low).

Category	Proposed Climate Tipping Element [& Tipping Point]*		Threshold (°C)			Timescale (years)			Maximum Impact** (°C)	
			Est.	Min	Max	Est.	Min	Max	Global	Region
Global 'Core' Tipping Elements	GrIS	Greenland Ice Sheet [collapse]	1.5	0.8	3.0	10 ky	1 ky	15 ky	0.13	0.5 to 3.0
	WAIS	West Antarctic Ice Sheet [collapse]	1.5	1.0	3.0	2 ky	500	13 ky	0.05	1.0
	LABC	Labrador Sea / SPG Convection [collapse]	1.8	1.1	3.8	10	5	50	-0.46	-3.0
	EASB	East Antarctic Subglacial Basins [collapse]	3.0	2.0	6.0	2 ky	500	10 ky	0.05?	?
	AMAZ	Amazon Rainforest [dieback]	3.5	2.0	6.0	100	50	200	Partial: ~30 GtC / ~0.06°C Total: ~75 GtC / ~0.15°C	1.0 to 2.0
	PFTP	Boreal Permafrost [collapse]	4.0	3.0	6.0	50	25	120	~264 GtC / ~369 GtCe / ~0.3-0.4°C	<
	AMOC	Atlantic M.O. Circulation [collapse]	4.0	1.4	8.0	100	15	300	-0.54	-4 to - 10
	AWSI	Arctic Winter Sea Ice [collapse]	6.3	4.5	8.7	20	10	100	0.60	~0.6 to 1.2
	EAIS	East Antarctic Ice Sheet [collapse]	7.5	5.0	10.0	10 ky<	10 ky	100 ky?	0.60	2.0
Regional 'Impact' Tipping Elements	REEF	Low-latitude Coral Reefs [die-off]	1.5	1.0	2.0	10	/	/	<	/
	PFAT	Boreal Permafrost [abrupt thaw]	1.5	1.0	2.3	200	100	300	+~25-50% for abrupt vs. gradual = ~5-10 GtC/7-14 GtCe/ 0.02-0.04°C per °C @2100; ~13-25 GtC/18-35 GtCe/ 0.05-0.11°C per °C @2300, up to max. ~100 GtC (~0.2°C) on top of gradual	
	BARI	Barents Sea Ice [abrupt loss]	1.6	1.5	1.7	25	/	/	<	+
	GLCR	Extra-polar Mountain Glaciers [loss]	2.0	1.5	3.0	200	50	1 ky	0.08	+
	SAHL	Sahel & W. African Monsoon [greening]	2.8	2.0	3.5	10	10	50	<	+
	BORF	Boreal Forest [southern dieback]	4.0	1.4	5.0	50	25?	100	+52GtC / net -0.08°C	~-1.0
	TUND	Boreal Forest [northern expansion]	4.0	1.5	7.2	50	40	100	-31 GtC / net +0.08°C	~-1.0

*Bolded element names indicates elements featured in previous climate tipping element characterizations.

**Feedback strength in $^{\circ}\text{C}$ per $^{\circ}\text{C}$ for abrupt permafrost thaw is calculated relative to pre-industrial and declines with further degrees of warming (by $\sim 21\%$ per $^{\circ}\text{C}$).

Supplementary Materials:

Materials and Methods

Supplementary Text

Tables S1-S4

References (101-200)

Data S1 (Climate Tipping Elements Database)

Supplementary Materials for: Updated assessment suggests >1.5°C global warming could trigger multiple climate tipping points

David I. Armstrong McKay^{1,2,3*†}, Arie Staal^{1,2,4}, Jesse F. Abrams³, Ricarda Winkelmann⁵, Boris Sakschewski⁵, Sina Loriani⁵, Ingo Fetzer^{1,2}, Sarah E. Cornell^{1,2}, Johan Rockström^{1,5}, Timothy M. Lenton^{3*}

Affiliations:

¹ Stockholm Resilience Centre, Stockholm University; Stockholm, Sweden.

² Bolin Centre for Climate Research, Stockholm University; Stockholm, Sweden.

³ Global Systems Institute, University of Exeter; Exeter, UK.

⁴ Copernicus Institute of Sustainable Development, Utrecht University; Utrecht, Netherlands.

⁵ Potsdam Institute for Climate Impact Research; Potsdam, Germany.

*david.armstrongmckay@su.se / d.mckay@exeter.ac.uk, t.m.lenton@exeter.ac.uk

† Current address: Georesilience Analytics; Leatherhead, UK.

This PDF file includes:

Materials and Methods

Supplementary Text

Tables S1 to S4

Caption for Data S1

Other Supplementary Materials for this manuscript include the following:

Data S1 (Climate Tipping Elements Database)

Materials and Methods

We mined the literature subsequent to (1), including studies of paleoclimate change, observed change, early warning signals, future model projections, underlying theory, and existing assessments, to draw up a longlist of possible candidate tipping elements (Table S3). For each we extracted information on evidence for self-perpetuation, temperature thresholds, hysteresis/irreversibility, transition timescales, and global/regional impacts on climate, which we then use subjective expert judgment to determine our best estimates. From this evidence (or lack of it) we drew up shortlists (Main text Table 1) of ‘core’ global tipping elements and regional ‘impact’ tipping elements (Main text Fig. 1), for which we summarize the rationale in the main text and below. Candidates that did not make the shortlists (Supplementary Table S3) are classed as: (a) ‘uncertain’ tipping elements – due to limited evidence for self-perpetuating feedback and threshold behavior; (b) ‘unlikely’ tipping elements – possessing only localized tipping or non-feedback response to climate change; and (c) ‘threshold-free feedbacks’ – where feedbacks are not strong enough to self-perpetuate. Different parts or phenomena of some systems – notably permafrost – are assigned to different categories. We give (high/medium/low) subjective levels of confidence in best estimate, minimum, and maximum temperature thresholds, timescales of transition, and global and local impacts on climate, based on the number and agreement of studies available to determine each estimate. We define crossing a CTP as ‘possible’ beyond its minimum temperature threshold and ‘likely’ beyond its best estimate. Differences to past lists of tipping elements are described in Supplementary Table S4.

Supplementary Text

Other climate tipping element candidates

Uncertain potential climate tipping elements

Southern Ocean sea-ice (SOSI). Several abrupt shifts in SOSI occur in CMIP5 models (18). Abrupt loss was detected in the Pacific and Atlantic Ocean sectors at $\sim 2.1^{\circ}\text{C}$ ($1.4\text{--}2.9^{\circ}\text{C}$) in two models, an abrupt increase occurred at $\sim 1.6^{\circ}\text{C}$ in the Indian Ocean sector in one model, and forced bimodal switches occurred in the Southern Ocean at $\sim 2.9^{\circ}\text{C}$ ($1.7\text{--}4.7^{\circ}\text{C}$) in two models. These shifts are likely feedback-driven and may be self-perpetuating, although further analysis is required to determine threshold dynamics. However, AR6 has only low confidence in past and future simulations for Antarctic sea ice due to model limitations (20). Hence, we include Southern Ocean sea ice as an uncertain potential regional/impact tipping element with limited global impacts, and best estimates of thresholds and timescales 25-50yr based on Drijfhout et al. (2015) [with low to medium confidence depending on number of models].

Tibetan Plateau Snow (TIBS). Abrupt snow melt on the Tibetan Plateau was detected in two CMIP5 models at $1.7\text{--}2^{\circ}\text{C}$ (18). Despite its abruptness, this abrupt melt is not driven by a self-perpetuating feedback. Instead, this nonlinear response to warming is a threshold mechanism related to a negative annual mass flux balance resulting from greater seasonality in snow cover. It also occurs in only two CMIP5 models. As a result, we categorize Tibetan Plateau snow melt as an uncertain tipping element.

Indian summer monsoon (INSM). Simple models suggest that the existence of a self-propelling moisture-advection feedback can result in two stable states (the current wet state and an alternative dry state) and threshold behavior for the South Asian monsoon (101, 102). Past research has suggested that if planetary albedo over South Asia becomes greater than 0.5 the INSM could collapse, based on the possible presence of multiple metastable regimes (102). However, more recently there has been debate as to whether this feedback is strong enough to give rise to alternative stable states (23, 103, 104). It is also uncertain as to whether a global warming threshold exists for INSM separate to pollution, with warming instead tending to counteract the aerosol effect and overall strengthening likely by 3°C (88, 105). We therefore categorize INSM as an uncertain potential tipping element with a non-GMST anthropogenic driver.

Indian Ocean Upwelling (IOUP). An abrupt but temporary increase in upwelling and an associated phytoplankton bloom occurs in one CMIP5 model at $\sim 10.9^{\circ}\text{C}$ (18). This is driven by self-amplifying increase in upwelling (initially triggered by increased wind stress and equatorial divergence) that delivers extra nutrients to the surface, but the reversal a few decades later makes it unclear as to what extent these feedbacks are self-perpetuating. If evidence emerged from several sources supporting the existence of this as a tipping point then IOUP would be categorized as a regional impact tipping element, but for now we categorize it as an uncertain potential tipping element.

Equatorial stratocumulus clouds (EQSC). In a recent model a positive feedback-driven abrupt breakup of equatorial stratocumulus clouds occurs at >1200 ppm atmospheric CO_2 ($1400\text{--}2200$ ppm in sensitivity analysis), which is equivalent to a GMST of 6.3°C ($7\text{--}8.9^{\circ}\text{C}$) (96). This results in a dramatic $\sim 8^{\circ}\text{C}$ increase in GMST ($\sim 10^{\circ}\text{C}$ in subtropics) in only ~ 10 years, and substantial model hysteresis indicates the existence of bistable states. However this has only been resolved in one model so far, and so remains highly

uncertain. If further research supports the existence of this tipping point, EQSC would constitute a serious global core tipping element, albeit one that is unlikely to be triggered by anthropogenic warming unless global policy fails.

Ocean Oxygenation (OCOX). A tipping threshold for weathered phosphorus input to the ocean triggering global ocean anoxia has been previously identified and was likely triggered multiple times during the Mesozoic era, with extreme consequences for the marine biosphere (1, 106, 107). However, the associated global warming level required to reach this phosphorous threshold is unclear, although it is likely that RCP8.5 would be sufficient if maintained for tens of millennia (106, 108, 109). We conclude that there is likely an oceanic anoxia tipping point that would have serious global consequences if triggered, but given the uncertainty around the climate forcing required we categorize ocean anoxia as an uncertain potential tipping element.

Antarctic Bottom Water / Southern MOC (AABW). The impact of Antarctic ice sheet meltwater on AABW formation is not resolved in most Earth system models, and did not feature in any CMIP5 model (110). However, observations suggest it may already be weakening, and collapse over ~50 years was found to be possible beyond a freshwater melt threshold (equivalent to 1.75-3°C GMST) in one model adapted to include this process (110). It is categorized as an uncertain potential tipping element, due to lack of models, but if confirmed it would likely act as a Global/Core tipping element as its collapse would have global consequences.

Cloud feedbacks (CLFB). Several recent models indicate that cloud feedbacks (specially over the Southern Ocean) could also transition to net-positive and amplify climate sensitivity beyond a threshold in the 3-5°C range (111–113). This could be a rare example of a global tipping point in that it markedly increases climate sensitivity from ~3°C to ~5°C global warming for each CO₂ doubling. However, the realism of these high-sensitivity models has been questioned (114, 115), and although it features a threshold it is unclear if this threshold results from tipping dynamics. We therefore categorize this as an uncertain potential tipping element, requiring further study to constrain.

Temperate forests (TEMF). Recent observations suggest that temperate forests are experiencing regional mortality increases as a result of heat stress, droughts, extreme weather, and insect outbreaks (116–124). Potential self-amplification might occur under increasing soil moisture deficits stemming from reduced forest cover which in turn influence precipitation regimes (125–128) and amplify local warming (129). However, it is unclear from theory or models whether temperate forests feature strong enough self-amplifying feedbacks to result in the same scale bistability associated with parts of the Amazon rainforest and boreal forest (130). As such, we categorize temperate forests as an uncertain potential regional impact tipping element.

Congo forest (CONG). The Congo rainforest has been proposed as a potential climate tipping element with similar possible tipping dynamics to the Amazon (e.g. Staal et al., 2020), but evidence of a specific tipping threshold across large parts of the forest is currently lacking. Furthermore, the regional forest-rainfall feedback in the Congo is weaker than in the Amazon. Bistability analysis indicates that currently the whole Congo rainforest lacks resilience against rainfall decline, but unlike the Amazon global warming may actually increase resilience and create larger uni-stable rainforest areas and a greater potential forest range (17). Conversely, this same analysis indicated that southeast Asian rainforests are not vulnerable to forest-rainfall feedback (as the climate zone is largely maritime across mainland and maritime southeast Asia) and is therefore not proposed as a potential climate tipping element.

Unlikely tipping elements

Arctic ozone hole (AOZH). Stratospheric ozone depletion has been driven by now-declining anthropogenic CFC emissions but can be enhanced by cooler temperatures. It has previously been suggested that global warming, which is associated with stratospheric cooling, could therefore lead to increased ozone destruction in polar regions by increasing polar stratospheric clouds and strengthening the polar vortex (19, 131–135). As ozone destruction itself also leads to cooling this could have potentially triggered an abrupt self-perpetuating expansion of the Arctic ozone hole, potentially seriously impacting Europe (19). However, stratospheric ozone is gradually recovering since the Montreal Protocol limited CFC emissions from 1987, and it is projected that a global warming-induced Arctic ozone hole expansion will become impossible beyond 2030–2060, although some uncertainties in the response of polar vortex behavior to high global warming levels remain (16, 19). As such, we categorize it is unlikely to be a tipping element unless a substantial breakdown in the Montreal Protocol occurs.

El Niño Southern Oscillation (ENSO). (1) identified ENSO as a potential tipping element on the basis that ENSO was possibly persistent during the Pliocene (~3°C above pre-industrial) and so could potentially tip in to a persistent-El Niño state with warming. Alternatively, it was posited that ENSO could tip to a higher amplitude regime (1). However, subsequent modelling has shown there is insufficient evidence for a sharp regime threshold for a more extreme or persistent ENSO, though increased rainfall amplitude variability is projected to increase with warming (21, 22). We therefore conclude that ENSO is unlikely to be a tipping element itself, although other tipping points might have substantial impacts on ENSO.

Northern Polar Jet Stream (JETS). It has been proposed that Arctic warming amplification has resulted in increasing instability of the Northern polar jet stream, leading to increased extreme weather events in Northern mid-latitudes (136). This led to the jet stream being included as a potential tipping element by Steffen et al. (2018), although no justification was given for the 3–5°C temperature threshold estimate. However, the link between Arctic amplification and mid-latitude weather trends has been challenged, with longer datasets suggesting the previous correlation may have been acausal (137). IPCC AR6 concluded that there was low agreement on mechanisms linking Arctic amplification and jet stream response (68) and low confidence on the contribution of Arctic warming to mid-latitude climate (138). As a result of this uncertainty and the lack of a proposed self-perpetuating feedback mechanism for jet stream instability we categorize the Northern polar jet stream as unlikely to be a tipping element.

Threshold-free feedbacks

Arctic summer sea ice (ASSI). As described in the main text, ASSI has been declining since the 1970s particularly since the 1990s, outpacing past IPCC projections (29). This decline is amplified by the ice-albedo feedback (sea ice retreat exposes darker water that absorbs more incoming solar energy), and might be further amplified by feedbacks to cloud cover, but negative feedbacks can act to prevent runaway sea ice loss (19). CMIP6 models better capture historical ASSI decline, and project occasional ice-free Septembers will occur above 1.5°C GMST, becoming common beyond 2°C and permanent around 3°C (30). However, current models suggest that it is unlikely to feature a tipping point beyond which loss would self-perpetuate (20). Hence, we re-categorize ASSI as a threshold-free feedback, adding ~0.25°C to global temperatures (139).

Marine methane hydrates (MMHD). Methane hydrates (also known as clathrates) are deposits of methane in subsea sediments that under high pressure and low temperature are locked in to ice-like structures. The widespread dissociation of subsea methane hydrates has previously been hypothesized as a major tipping element in the climate system that may have previously driven the Eocene hyperthermal events (140–145). As such, it has been suggested that anthropogenic warming, which is projected to be of a similar magnitude but faster rate if unabated, could also trigger hydrate dissociation (1, 140, 146). However, more detailed mechanistic modelling of the response of hydrates to warming suggests a lag of 100s-1000s of years between warming and methane release due to latent heat slowing heat propagation and the loss of much of the released methane during sediment transport processes (143). There is also no clear mechanism for hydrate dissociation to be able to self-perpetuate independently of thermal forcing, with latent heat processes instead resisting rather than amplifying thermal propagation through hydrate deposits. Instead, hydrates may have more likely acted as a gradual feedback during events like the PETM, helping to amplify and lengthen the hyperthermal rather than causing the abrupt initial warming itself (147, 148). As hydrates are scattered around the Earth's continental shelves and slopes in isolated deposits they are unlikely to trigger each other, but if deposits were concentrated around a particular depth then ocean warming could hypothetically trigger synchronous dissociation and release that could amount to a threshold-like response. However, no such depth concentration is known, and ocean warming and hydrate dissociation are slow enough processes to smooth out any release. Instead, smaller shallow hydrate deposits are expected to gradually begin to dissociate and release methane in to the overlying ocean in the next few centuries under higher warming scenarios while larger deep deposits remain relatively stable until much later (149). IPCC AR6 projects a minimal release of hydrate-derived methane in the 21st Century, with a maximum increase in atmospheric methane of ~20 ppb (54). Based on the evidence that hydrate dissociation likely does not independently self-perpetuate beyond a clear global threshold, we categorize methane hydrates as a long-term threshold-free feedback that will somewhat amplify the future stabilized global warming level on geological timescales.

Gradual permafrost thaw (PFGT). Permafrost is permanently frozen soil containing substantial organic carbon deposits, and its thaw with global warming leads to the respiration and release of this carbon as CO₂ and methane (52). As described in the main text, gradual permafrost thaw (PFGT) decay is observable in modern and palaeo records beyond 1-1.5°C (52–54, 150) and in several models acts as a potentially nonlinear but threshold-free feedback (151–157). We summarize the literature (Table S3) as indicating that gradual thaw processes act as a threshold-free feedback that becomes widespread by 1.5°C (1-2.3°C) [high confidence], occurring over a timescale of 200y (100-300y) [medium confidence], with emissions of ~20-50GtC at 2100-2300 respectively per degree of warming (~0.09-0.21°C per °C at pre-industrial, including ~40% amplification by methane (52)). Abrupt thaw processes such as thermokarst lake formation or slope slumping also occur alongside gradual thaw and release additional CO₂ and methane emissions (55, 158) which we classify as a regional impact tipping element, and potential wide-scale collapse as a result of abrupt drying and the heat-generating 'compost bomb' instabilities in particularly carbon-rich permafrost (16, 18, 56, 58, 59) as a global core tipping element (see main text).

Ocean biological pump and ocean carbon sink (PUMP). The ocean takes up around a quarter of all human CO₂ emissions, making it a substantial carbon sink (159). While this mostly driven by the 'solubility pump' (i.e. direct dissolution of CO₂ in to seawater), the flow of carbon from surface to deep

ocean is modulated by the ‘biological pump’ (160). This describes the drawdown of CO₂ from the surface ocean in to marine biomass and the export of this biomass in to the deep ocean, where it remains for several centuries. This export is weakening in response to climate change, with warming leading to the expansion of low-nutrient ‘oligotrophic’ regions and a shift to smaller-sized plankton that produce less exportable carbon, slightly reducing the capacity of the ocean carbon sink (161, 162). The biological pump has been presented by some as a potential tipping element (e.g. <https://www.pik-potsdam.de/en/output/infodesk/tipping-elements/kippelemente>), but there is no known self-perpetuation mechanism that enables its decline to become independent of climate forcing, and in models the changes scale quasi-linearly with emission scenario (162). The solubility pump also declines with warming (as warmer water can dissolve less CO₂) but like the biological pump also has no known tipping behavior, leading to an eventual peak but not the reversal of the overall ocean carbon sink in the latest CMIP6 models (54). Potential ocean tipping points mostly consist of ecosystem regime shifts in response to warming or acidification rather than for ocean carbon storage in general (163). It has been hypothesized that there may be a reachable threshold for carbon release rate in to the ocean carbon cycle that could trigger a more substantial carbon cycle disruption like in previous mass extinction events (164, 165), but this relies on a highly simplified model and remains speculative. As such, we categorize the warming-induced decline of the ocean biological pump (and the ocean carbon sink in general) as threshold-free feedbacks rather than tipping points, although nonlinear behavior cannot be fully ruled out.

Land carbon sink (LAND). Alongside the ocean carbon sink, the terrestrial biosphere takes up around another quarter of human CO₂ emissions, mostly as a result of higher CO₂ concentrations leading to more productive plants (the ‘CO₂ fertilization’ effect) (159). However, increasing temperatures, droughts, and nutrient limitations will eventually limit how much CO₂ the land biosphere can take up, leading to a reduced fraction of emitted CO₂ being drawn down and eventually to a transition from net carbon sink to net carbon source after 2100CE (54). Projections of the future global land sink vary widely though as a result of missing model processes such as nutrient limitation or vegetation dynamics, leading to low agreement in AR6 on the timing and eventual magnitude of this transition. Recent observations indicate that land carbon sink slowdown may have already begun after 2000CE (~0.7°C) and entered decline since ~2015CE (~1.0°C), while another analysis of observations suggests CO₂ fertilization began to decline above as low as ~0.3°C and may reach zero beyond ~1.2°C (166). This suggests that models are overestimating CO₂ fertilization and underestimating land carbon sink slowdown, in particular in the boreal region (167, 168). The carbon sink of individual ecoregions and biomes such as tropical forests are already declining in some cases, with for example the Amazon’s carbon uptake rate declining beyond ~0.5°C, projected to become a net sink by ~1.5°C, and in combination with deforestation the south-eastern likely a net source already (14, 169–171). Parts of the Amazon and the Boreal forests may also have tipping points beyond which a regime shift and therefore carbon storage capacity substantially shifts (76, 83). At a global scale though these changes are currently compensated by other still active land sinks increasing instead, with for example boreal and tundra greening compensating for the decline in the tropical sink (172). While a global sink-to-source transition will occur at some point, for example as a result of photosynthesis rates peaking and falling in sub-tropical ecoregions while respiration rates continue to increase (173), this transition is not a tipping point in itself as it is a gradual shift in feedback strengths which is not self-perpetuating. Based on these lines of evidence, we categorize the land carbon sink as a threshold-free feedback, although nonlinear behavior is still probable.

Other potential tipping elements or feedbacks

There are a number of other potential climate tipping points suggested or implied by the literature, for example aridification of inner East Asia (174), forest colonization of non-frozen peatlands (175), and soil organic carbon (176). However, there is currently insufficient evidence to classify them or determine their potential thresholds and impacts, and so we leave them out of this current assessment.

Climate Impact Estimates

In this section we explain how we arrived at some of the climate impact estimates in the main text for numbers that were not directly acquired or averaged from the literature.

Amazon dieback: Total above-ground biomass (AGB; ~ 70 GtC, i.e. ~ 127 MgC/ha), below-ground biomass (BGB; ~ 21 GtC, assuming relationship of (177)), and soil carbon (60-110 GtC – approximately similar to biomass) amounts to 150-200 GtC (3, 72, 73, 178). If all of the Amazon was converted to degraded secondary forest or savannah and we assume an AGB density of ~ 20 MgC/ha (based on repeatedly burnt secondary forest in (179) and neighboring Cerrado savannah (180, 181)) and constant soil carbon (as soil carbon response to deforestation is more complex, and can even increase (182)) then AGB would decline to ~ 11 GtC and BGB to ~ 4 GtC, releasing ~ 75 GtC to the atmosphere (causing a global warming of $\sim 0.1^\circ\text{C}$, plus $\sim 0.05^\circ\text{C}$ biogeophysical feedbacks as approximately half of tropical forest biomass loss in (183)). A partial $\sim 40\%$ dieback (matching current bistable area (17, 75, 184, 185)) would therefore release ~ 30 GtC ($\sim 0.06^\circ\text{C}$).

Boreal forest dieback/expansion: Steffen et al. (2018) estimate that $\sim 50\%$ boreal forest dieback would lead to ~ 52 GtC release ($\sim 0.06^\circ\text{C}$ global warming at tipping threshold of 4°C) based on the difference between estimated boreal forest and temperate grassland carbon densities. Pan et al. (2011) estimated boreal forests contain ~ 109 GtC in biomass (~ 54 GtC) and deadwood, litter, etc. (~ 54 GtC) (and ~ 163 GtC in soil carbon), while Bradshaw and Warkentin (2015) estimated 65-195 GtC for total vegetation biomass including deadwood, and Thurner et al. (2014) estimated ~ 41 GtC in live biomass. In contrast, arbitrary total boreal deforestation by (183) released only ~ 8 GtC, and a linear scaling of the latest IPCC estimate for potential boreal forest loss carbon release yields ~ 35 GtC at 4°C (54, 83). Despite the wide range in boreal forest carbon storage and release estimates, we take ~ 100 GtC as a plausible upper bound for total losable biomass, including above and below-ground biomass and deadwood but ignoring potential soil carbon change, and keep ~ 52 GtC as our 50% boreal dieback estimate. Biogeophysical-only effects for total dieback are estimated at $\sim 0.28^\circ\text{C}$ global cooling (183), half of which would result in a net global cooling of $\sim 0.08^\circ\text{C}$ when combined with the carbon release above.

Fewer estimates are available for carbon uptake due to boreal forest expansion into the boreal tundra, but ~ 13 GtC has been projected for total boreal afforestation (183) and IPCC AR6 estimating a similar value for boreal expansion carbon uptake as for boreal forest dieback carbon release (~ 21 GtC scaling to 4°C (54, 83). Furthermore, forest expansion also results in counteracting biogeophysical feedbacks (adding 0.3°C to global warming for total boreal afforestation (183)). We crudely estimate that boreal forest expansion across $\sim 50\%$ of its potential range would result in a ~ 31 GtC biomass sink ($\sim -0.04^\circ\text{C}$ at 4°C), which combined with biogeophysical feedbacks yields a $\sim 0.08^\circ\text{C}$ net global warming. This approximately balances out warming from dieback on the southern edge of the boreal forest biome, but regional effects and nonlinear interactions will be non-negligible.

Both boreal forest dieback and expansion also have complex and poorly quantified interactions with permafrost thaw (52). In some regions thaw can lead to forest loss and wetland formation (189, 190). Boreal forest disturbances like wildfires are likely to accelerate permafrost thaw in some but not all ecosystems (191–193). Regional warming of up to $\sim 1^\circ\text{C}$ from forest expansion (183) could potentially accelerate permafrost thaw in tundra regions, which could either restrict or enhance further forest expansion depending on whether thaw leads to localized wetting or drying (56, 189, 190). In this

assessment we focus on climate drivers rather than ecological interactions to produce independent estimates for each element, but note that these interactions add uncertainty and require further study to constrain.

Permafrost thaw/collapse: For gradual permafrost thaw (PFGT), we subjectively judge a central estimate reflecting the assessed literature. We estimate a feedback strength of ~ 20 GtC ($\sim 0.09^\circ\text{C}$ from a pre-industrial baseline) released per degree of global warming at 2100 (when many studies evaluate permafrost feedback strength at; IPCC AR6 (54) estimated ~ 18 GtC, Schuur et al. (2015) implied ~ 21 GtC), increasing to ~ 50 GtC ($\sim 0.21^\circ\text{C}$) by 2300, reflecting that the majority of emissions likely occurs after 2100 ($\sim 59\%$ in Schuur et al. (2015)). The assessed studies range from 10 to 27 GtC (~ 0.04 to $\sim 0.12^\circ\text{C}$) per $^\circ\text{C}$ for the former (reflecting the IPCC AR6 5th-95th percentile range of 3-41 GtC), and 30 to 68 GtC (~ 0.13 to $\sim 0.29^\circ\text{C}$) per $^\circ\text{C}$ for the latter. The above temperature figures also include a $\sim 40\%$ amplification due to methane (assuming $\sim 2.3\%$ of carbon is emitted as methane based on Schuur et al. (2015)), although some studies suggest a smaller amplification by methane (e.g. 10-18% amplification in Koven et al. (2013), and even less in de Vrese et al. (2021) where methane is estimated to account for only $\sim 0.2\%$ of carbon emissions). These estimates exclude carbon uptake by surface vegetation growth, which partly or wholly offsets permafrost carbon losses in some studies (e.g. McGuire et al., 2018) but is far less in others (e.g. de Vrese et al., 2021), with complex ecological interactions making the response highly uncertain.

For abrupt permafrost thaw (PFAT), it has previously been suggested that abrupt thaw processes (such as slope slumping, thermokarst lake formation, erosion gullies, etc.) could up to double permafrost emissions from gradual thaw (158). Turetsky et al. (2020) estimate ~ 80 GtC of permafrost carbon emissions due to abrupt thaw by 2300, amounting to a feedback of ~ 2.3 - 3.1 GtC per $^\circ\text{C}$ from 2000 to 2100 (RCP4.5-8.5) and ~ 7.2 - 11.6 GtC per $^\circ\text{C}$ from 2100 to 2300 (RCP8.5-4.5 – note that emissions are greater for RCP4.5 in long-term, indicating nonlinearity). Along with an elevated warming amplification by methane of 100% (from methane reaching $>20\%$ of carbon emissions) this results in a global warming feedback of ~ 0.01 - 0.02°C per $^\circ\text{C}$ by 2100 (RCP4.5-8.5) and ~ 0.04 - 0.07°C per $^\circ\text{C}$ by 2300 (RCP8.5-4.5). This represents an extra 16-33% warming beyond the gradual thaw estimates above. This is lower than the $\sim 100\%$ extra sometimes suggested as the gradual thaw emission estimates used for comparison in Turetsky et al. (2020) were on the low side compared to the literature range assessed earlier (~ 70.8 GtCO₂ / ~ 19.2 GtC in 2000-2100 for RCP8.5, i.e. ~ 4.8 GtC per $^\circ\text{C}$, in Turetsky et al. (2020), versus ~ 57.4 GtC in 2010-2100 for RCP8.5, i.e. ~ 17 GtC per $^\circ\text{C}$, based on the study (196) cited by Turetsky et al. (2020), and our estimate of ~ 20 GtC per $^\circ\text{C}$). Schuur et al. (2015)'s expert judgement raised their estimate for permafrost carbon emissions from ~ 92 GtC from modelled gradual thaw to 130-160 GtC when accounting for unresolved processes, implying a 41-74% amplification by abrupt thaw processes. However, interactions of abrupt thaw processes with abrupt drying and carbon-rich Yedoma deposits could produce even more emissions in some regions (see PFTP discussion below).

For permafrost collapse (PFTP), we assume that 50% of Yedoma domain carbon (~ 400 GtC (57)) and permafrost in regions subject to abrupt drying beyond $\sim 4^\circ\text{C}$ (2.2 Mkm² (56), $\sim 10\%$ of total permafrost area of ~ 21 Mkm² (20, 197, 198) which would contain ~ 108 GtC in the top 3m (52) if scaled linearly) decomposes over 50 years (assuming drying (56) leads to enhanced decomposition (52, 199, 200) and fast thaw processes make deep Yedoma accessible (52, 57)), releasing up to ~ 254 GtC ($\sim 0.3^\circ\text{C}$ warming if released as CO₂ at $\sim 4^\circ\text{C}$ of warming; partial release as methane can amplify by $\sim 40\%$ (155) to $\sim 0.4^\circ\text{C}$).

Supplementary Tables and Data

(see overleaf)

Table S2. Comparing past climate tipping element characterizations and abrupt events detected in CMIP5. Red boxes indicate thresholds <2°C (i.e. accessible within Paris range), yellow 2-5°C (accessible in next century), and green >5°C (only in long-term with very high emissions/sensitivity).

Proposed Climate Tipping Element [& Tipping Point]	Past Climate Tipping Element characterizations												CMIP5 Abrupt Events		
	Lenton et al. (2008)			Schellnhuber et al. (2016)			Steffen et al. (2018)			Lenton et al. (2019)			Drijfhout et al. (2015)		
	Thresh- old (°C)	Time (y)	Impact (°C)	Thresh- old (°C)	Time (y)	Impact (°C)	Thresh- old (°C)	Time (y)	Impact (°C)	Thresh- old (°C)	Time (y)	Impact (°C)	Thresh- old (°C)	Time (y)	Impact (°C)
Arctic Summer Sea Ice [loss] (ASSI)	0.5-2	10	+	0.8-2.5			1-3		+	2<	-	+ reg.	Rapid ice melt feedbacks not well represented		
Greenland Ice Sheets [collapse] (GRIS)	1-2	>300	<	0.8-3.2			1-3		+	1.5	1k-10k				
West Antarctic Ice Sheet [collapse] (WAIS)	3-5	>300	<	0.8-5.5			1-3		+	1-1.5	100-1ks				
Atlantic M.O. Circulation [collapse] (AMOC)	3-5	100	- reg	3.5-5.5			3-5		+/-reg.?	N/A		+/- reg.	1.6*	50	-4 reg.
Amazon Rainforest [dieback] (AMAZ)	3-4	50	<	3.5-4.5			3-5		+0.05@2	N/A		+	2.5/6.2	150	
Boreal Forest [southern dieback] (BORF)	3-5	50	<	3.5-5.5			3-5		+0.06@2	N/A		+	Limited veg. dynamics		
Boreal Permafrost [collapse] (PFTP)	N/A	<100	+	4.8-9+			5+		+1 @2C	N/A		+	5.6	50	
Sahel & W. African Monsoon [greening] (SAHL)	3-5	10	<	3.5-5.5			3-5		<?	N/A			2.8	50	
El Niño [permanent/extreme] (ENSO)	3-6	100	<	3.5-7.0			3-5		+(reg.)?						
Low-latitude Coral Reefs [die-off] (REEF)				1.3-1.8?			1-3		<?	<2			Not represented		
East Antarctic Ice Sheet [collapse] (EAIS)				4.5-9+			5+		+?				Timescale not modelled		
Arctic Winter Sea Ice [collapse] (AWSI)				5.5-9+			5+		+?				6.3	100	+ reg.
Extra-polar Mountain Glaciers [loss] (GLCR)				1-2.6			1-3		<?						
Northern Polar Jet Stream [instability] (JETS)							3-5		<?						
Indian Summer Monsoon [collapse] (INSM)	N/A	1	<				3-5		<?	N/A					
Ocean Oxygenation [global anoxia] (OCOX)	N/A	10k	<												
Arctic Ozone Hole [abrupt expansion] (AOZH)	?	<1	<												
Antarctic Bottom Water [collapse] (AABW)	?	100	<												
Marine Methane Hydrates [dissoc.] (MMHD)	?	1k-100k	+				N/A	1ks	+0.5						
Boreal forest [northern expansion] (TUND)	N/A	100	+										7.2	100	+ reg.
SO sea ice [bimodality] (SOSI-Bi)													2.9	50	/
IO upwelling [increase] (IOUP)													10.9	25	/
Barents sea ice [loss] (BARI)													1.6	25	+ reg.
SO sea ice [loss] (SOSI-AP)													2.1	25	+ reg.
SO sea ice [increase] (SOSI-In)													1.6	25	- reg.
Labrador Sea Convection [collapse] (LABC)													1.7	10	- reg.
Tibetan Plateau Snow [abrupt loss] (TIBS)													1.8	25	+ reg.
Equat. Stratocumulus Clouds [breakup] (EQSC)										~6.3		8			
Ocean Biological Pump [weaken] (PUMP)							N/A	FB	0.02@2						
Global Land Carbon Sink [weaken] (LAND)							N/A	FB	0.25@2						

Table S3. Summary of abrupt events detected in CMIP5 by Drijfhout et al. (2015). Colors for GMST thresholds indicate tipping points occurring below 2°C (red), between 2 and 5°C (yellow), and above 5°C (green). Bolded Abrupt Event names indicate phenomena that have previously been characterized as climate tipping points.

CMIP5 Abrupt Event*	Global Mean Surface Temperature (°C) the abrupt change occurs at:				No. models found in
	Mean	RCP8.5	RCP4.5	RCP2.6	
SO Sea ice bimodality (forced)	2.9	4.7	2.1		2
IO Upwelling change	10.9	10.9			1
Arctic winter sea ice collapse	6.3	6.3			5
Barents Abrupt sea ice loss	1.6	1.6			2
SO Abrupt sea ice loss	2.1	2.6	1.9	1.4	2
SO Abrupt sea ice increase	1.6		1.6		1
Labrador Sea Convection collapse	1.9	3.8	1.6	1.5	4
NA AMOC-induced collapse	1.6	1.9	1.6	1.4	1
Permafrost collapse	5.6	5.6			1
Tibetan Snow Melt	1.8	2.0	1.7		2
E. Sahel Vegetation changes	2.8	3.5	2.8	2.1	1
Boreal Forest expansion	7.2	7.2			1
Amazon Forest dieback	4.4	2.5-6.2			2

*Bold = also featured in past CTE characterizations

Table S4. Summary Table of literature-based estimates for thresholds, timescales, impact, activation time, self-perpetuation, rate-dependence, and hysteresis (see Materials and Methods for details). Colors for element acronyms represent Earth system domains (blue = cryosphere; green = biosphere; orange = ocean/atmosphere), all other colors represent confidence (red = low confidence; yellow = medium confidence; green = high confidence).

Category	Proposed Climate Tipping Element [& Tipping Point]*		Threshold (°C)			Timescale (years)			Max. Impact** (°C)		Activation Time	Dynamics			Comments
			Est.	Min	Max	Est.	Min	Max	Global	Region		Self-perp-et.?	Rate-dep-end.?	Hyst-eresis ?	
Global 'Core' Tipping Elements	GrIS	Greenland Ice Sheet [collapse]	1.5	0.8	3.0	10ky	1ky	15k y	0.13	0.5 to 3.0	?	Y	N	Y	GrIS has partially or fully collapsed over long millennial timescales in previous warm interglacials within the Paris Agreement Target range, with some models also supporting a tipping threshold (and significant hysteresis) in this range. IPCC express uncertainty on tipping below 3°C, but indicates collapse beyond 3°C is likely.
	WAIS	West Antarctic Ice Sheet [collapse]	1.5	1.0	3.0	2ky	500	13k y	0.05	1.0	60?	Y	N	Y	WAIS has partially or fully collapsed over millennial timescales in previous warm interglacials within the Paris Agreement Target range, with some models showing current or near-future warming sufficient to trigger collapse; some observations indicate some glaciers have already passed their local thresholds. Faster collapses within coming centuries possible beyond 2°C. Features clear potential self-perpetuation mechanisms (either MISI or MICI).
	LABC	Labrador Sea / SPG Convection [collapse]	1.8	1.1	3.8	10	5	50	-0.46	-3.0	?	M	M	M	Labrador Sea / North Atlantic SPG convection collapse is resolved by multiple CMIP5 models, and has strong regional consequences. Effectively a branch of AMOC with marginally smaller consequences but a much lower warming threshold in models that do resolve it.
	EASB	East Antarctic Subglacial Basins [collapse]	3.0	2.0	6.0	2ky	500	10k y	0.05?	?	200?	Y	P	Y	Consists of Wilkes, Aurora, and Recovery Basins. Marine-based like WAIS and unlike rest of EASIS, but thresholds are higher than WAIS. Wilkes has range of ~2-6C, and Aurora & Recovery ~6-8C. Partly depends on MICI feedback which is still debated, though is also partly vulnerable to MISI and so still has a self-perpetuation mechanism.

	AMAZ	Amazon Rainforest [dieback]	3.5	2.0	6.0	100	50	200	Partial: ~30 GtC / ~0.06°C Total: ~75 GtC / ~0.15°C	1.0 to 2.0	5-50	Y	P	Y	Partial bistability amplified by moisture recycling provides a clear self-perpetuation mechanism. However, there is also a strong non-climate driver in deforestation that makes dieback more likely, complicating temperature threshold estimation (our estimates assume climate-only forcing, and so are likely over-estimates). Total dieback (assuming most Amazon becomes bistable by ~4°C) = 75 GtC released (0.15-0.2°C, including biogeophysical feedbacks), partial dieback (~40% currently bistable, S. & E. Amazon) = 30 GtC (~0.06°C).
	PFTP	Boreal Permafrost [collapse]	4.0	3.0	6.0	50	25	120	~264 GtC / ~369 GtCe / ~0.3-0.4°C	<	?	Y	P	P	Warming beyond 4°C may risk wide scale abrupt drying regime shifts followed by self-perpetuating thawing in carbon-rich High Arctic & Yedoma regions (the "compost bomb"). The exact carbon pool vulnerable to drying/compost bomb instabilities is uncertain, so our estimate here assumes 50% C loss over 100y in Yedoma domain (~400 GtC [Strauss et al., 2017]) & Teufel et al. (2019) abrupt drying area (2.2M sqkm = 12% PF area = ~127 GtC [Schuur et al., 2015]). This instability is subject to hysteresis as soil C would take a long time to reform if climate were to cool, and has partial rate-dependence as although the "compost bomb" is rate-dependent itself abrupt drying could abruptly induce collapse instead.
	AMOC	Atlantic M.O. Circulation [collapse]	4.0	1.4	8.0	100	15	300	-0.54	-4 to -10	?	Y	P	M	Palaeo data and simple models suggest AMOC bistability and tipping thresholds, but CMIP models do not tend to resolve AMOC collapse. However, CMIP models are likely under-sensitive and do not include e.g. GrIS runoff effects. A runoff threshold is moderately likely (~0.1-0.5 Sv) but associated GMST highly uncertain; rate-dependence at lower end of range (0.1-0.3 Sv) is also likely but uncertain. Overshoot may be possible, but the exceedance time of Ritchie et al. (2021) doesn't match faster timescales (likely depends on assumption). May not be fully hysteretic as in some models the AMOC recovers when GRIS forcing declines (i.e. AMOC collapse is a response to GrIS rather than to global warming directly).

	AWSI	Arctic Winter Sea Ice [collapse]	6.3	4.5	8.7	20	10	100	0.60	~0.6 to 1.2	<10	M	N	M	Unlike ASSI, AWSI features a threshold prior to abrupt feedback-driven decline in CMIP5 models, which may be hysteretic. Regional warming scaled from ASSI by global impact ratio.
	EAIS	East Antarctic Ice Sheet [collapse]	7.5	5.0	10.0	10ky<	10ky	100ky?	0.60	2.0	?	M	N	Y	The land-based EAIS is subject to strong hysteresis that protects EAIS above its formation temperature (~5°C); very gradual melt back projected, self-amplified by elevation feedback although unclear if fully self-perpetuating.
Regional 'Impact' Tipping Elements	REEF	Low-latitude Coral Reefs [die-off]	1.5	1.0	2.0	10	/	/	<	/	?	L/P	M	P	70-90% warm-water coral reef loss is likely at ~1.5°C, with ~99% loss likely by 2°C. Partial hysteresis/self-perpetuation results from bleached reefs being irrecoverable directly, but new reefs can re-grow below threshold. There may be some rate dependence as slower warming rate may be adaptable to through ecosystems shifts to thermally-adapted species/taxa.
	PFAT	Boreal Permafrost [abrupt thaw]	1.5	1.0	2.3	200	100	300	+~25-50% for abrupt vs. gradual = ~5-10 GtC/7-14 GtC/0.02-0.04°C per °C @2100; ~13-25 GtC/18-35 GtC/0.05-0.11°C per °C @2300, up to max. ~100 GtC (~0.2°C) on top of gradual		?	L	P	P	Where a wide-scale compost bomb-type instability or abrupt drying is unlikely, permafrost thawing is likely to act as a threshold-free distributed feedback semi-proportional to global warming (with non-linearities). Abrupt thaw processes not yet in models (e.g. thermokarst lakes, slumping, etc.) add an extra 5 to 20 GtC/°C (0.02-0.06°C/°C) at 2100-2300 (i.e. ~25% extra) in Turetsky et al. (2020) and ~50% extra in Schuur et al. (2015)'s expert judgement; very fast (RCP8.5) suppresses CH4 & total feedback over longer timescales. Palaeorecords & models indicate both gradual & abrupt wide-scale thaw starts by ~1.5°C & in RCP2.6-4.5.
	BARI	Barents Sea Ice [abrupt loss]	1.6	1.5	1.7	25	/	/	<	+	?	M	N	?	CMIP5 Abrupt Event catalogue shows abrupt loss of winter sea ice in Barents Sea region (resulting from a positive feedback-driven shift in sea ice state) with significant impacts on regional weather
	GLCR	Extra-polar Mountain Glaciers [loss]	2.0	1.5	3.0	200	50	1000	0.08	+	?	L/P	N	N	Not a global tipping point, with each glacier having local thresholds & elevation feedbacks. 1.5°C leads to semi-stabilization by 2100 in many small glacier regions (but long-term survival not guaranteed), jump in loss by 2100 in RCP4.5/6.0 & Clark et al. (2016) suggests widespread small glacier losses

															expected to be committed at ~2°C, satisfying our synchronous localized tipping across sub-continental areas requirement. High Mountain Asia threshold might be a bit higher / take longer, but "peak water" (and therefore societal impacts) are reached at ~2°C.
	SAHL	Sahel & W. African Monsoon [greening]	2.8	2.0	3.5	10	10	50	<	+	?	M	N	M	Recent models suggest further global warming will lead to overall stronger WAM, leading to drying in WA and wetting in parts of Sahel, likely leading to greening & forest expansion in current grasslands including in Sahel that might be self-perpetuating and hysteretic to some degree. However, existence of tipping threshold for WAM and/or Sahel greening is uncertain, but based on evidence for regime shifts in palaeo data we maintain Sahel/WAM as a likely regional tipping element.
	BORF	Boreal Forest [southern dieback]	4.0	1.4	5.0	50	25?	100	+52GtC / net -0.08°C	~-1.0	?	M	M	Y	More likely to occur as localized dieback rather than a large swathe all at once, but widespread synchronous dieback is likely at higher warming (and is possibly rate-dependent). Current DGVMs may under-predict dieback (Koven, 2013), and there are substantial uncertainties around the relative effect of CO2 fertilization and nutrient limitation in models. Boreal dieback would predominantly cause global/regional cooling despite carbon release due to biogeophysical feedbacks - here we assume 50% loss C & albedo for our impact estimate.
	TUND	Boreal Forest [northern expansion]	4.0	1.5	7.2	50	40	100	-31 GtC / net +0.08°C	~1.0	?	M	N	M	Threshold uncertain with a wide range, but warming impact likely despite carbon sink gain due to self-amplifying positive biogeophysical feedbacks; warming estimated by scaling dieback value from Koven (2013) & assuming 50% C gain & albedo (Bathiany et al., 2010); possible hysteresis and self-amplification from tree cover maintaining local warmth, but unclear if self-amplification sufficient to become self-perpetuating
Threshold-free nonlinear feedbacks, or only	PFGT	Boreal Permafrost [gradual thaw]	1.5	1.0	2.3	200	100	300	20 GtC/28 GtCe/0.09°C per °C @2100; 50 GtC/70 GtCe/0.21°C per °C		?	N	P	P	Where a wide-scale compost bomb-type instability or abrupt drying is unlikely, permafrost thawing is likely to act as a threshold-free distributed feedback semi-proportional to global warming (with non-linearities). For gradual thaw, approx. 90GtC by 2100 RCP8.5 =>

localized non-synchronous tipping								@2300, up to max. ~260 GtC (~0.73°C)						20 GtC/°C => 0.09°C/°C (inc. +40% from CH4), & 60% of total emissions after 2100 => 50 GtC/°C & 0.21°C/°C total (up to a max. of ~0.73°C, accounting for decline in forcing strength at higher GWLs). Palaeorecords & models indicate both gradual & abrupt wide-scale thaw starts by ~1.5°C & in RCP2.6-4.5.	
	ASSI	Arctic Summer Sea Ice [loss]	2.0	1.3	2.9	20	10	50	0.25	0.25 to 0.5	N/A	N	N	N	ASSI is best represented as a threshold-free feedback as it lacks self-perpetuation (due to countering negative feedbacks) or hysteresis; it would semi-linearly regrow if GW was reversed (in contrast to AWSI).
	LAND	Global Land Carbon Sink [weaken]	2.0	1.0	3.5	?	/	/	>0.13°C per °C	/	N/A	L	M	L	Collectively the decline of the terrestrial carbon sink behaves as a threshold-free feedback with no clear global threshold featuring a self-perpetuation mechanism (although a sink-to-source transition threshold is likely) - our threshold estimates instead demarcate the point beyond which there is significant sink decline. Observations suggest weakening is occur faster than in models, implying models over-estimate the net effect of CO2 fertilization versus nutrient limitation or similar. Total impact is uncertain due to wide model spread and missing processes, and a faster rate would likely yield greater decline due to biome migration lag. Declining C sinks with increasing temperature/CO2 leads to more CO2 in atmosphere per unit emission, but simultaneously this CO2 has less effect at higher CO2 baselines (i.e. C sink weakening is counteracted by logarithmic greenhouse effect) and so counters C sink decline to some extent.
	PUMP	Ocean Biological Pump [weaken]	N/A	/	/	N/A	/	/	5GtC / 0.01°C per °C	/	N/A	N	N	N	There is no known tipping dynamics or nonlinear threshold for the ocean biological pump, and so we class it as a threshold-free feedback with a magnitude 2-6GtC per °C (provisional estimate 5GtC/°C). A highly simplified mathematical models have suggested that the ocean carbon sink as a whole (which the biological pump modulates) may have thresholds for massive carbon injections into

															ocean-atmosphere system [Rothman, 2017, 2019], but this remains hypothetical.
	MMH D	Marine Methane Hydrates [dissociation]	2.0?	/	/	1ky<	1ky	5ky	<0.5	/	100	N	M	P	A threshold for clathrates is uncertain - more likely to globally act as a threshold-free feedback as not self-perpetuating in itself. Max. impact based on Archer et al. (2009) is generous due to simplistic hydrate representation. Possibly subject to hysteresis as takes a long time for hydrates to "recharge" after global re-cooling, and possible rate-dependence for overcoming methane-degradation at higher production rates. For 21st Century clathrate impact is effectively zero (only relevant on millennial timescales).
Uncertain Potential Tipping Elements	INSM	Indian Summer Monsoon [shift]	N/A (only if AMOC collapses)			?	1	100	<	?	10-100?	M	N	M	Uncertain as to whether a global warming threshold exists for INSM separate to e.g. pollution, with warming instead tending to the counteract pollution effect and strengthen the monsoon. Global monsoon tipping/irreversible change only projected if AMOC collapses, in which case it would be an abrupt response to a different tipping point.
	SOSI-In	South. Ocean Sea Ice [Ind. increase]	1.6	/	/	25	/	/	<	-	?	M	N	?	CMIP5 Abrupt Event catalogue indicate a positive feedback-driven abrupt increase in Southern Ocean sea ice in the Indian Ocean sector, but IPCC AR6 has low confidence in SOSI model projections due to significant model limitations in this region.
	SOSI-AP	South. Ocean Sea Ice [Pac./Atl. loss]	2.1	1.4	2.9	25	/	/	<	+	?	M	N	?	CMIP5 Abrupt Event catalogue indicate a positive feedback-driven abrupt decrease in Southern Ocean sea ice in the Atlantic & Pacific Ocean sectors, but IPCC AR6 has low confidence in SOSI model projections due to significant model limitations in this region.
	SOSI-Bi	South. Ocean Sea Ice [bimodality]	2.9	1.7	4.5	50	/	/	<	+/-	?	M	N	M	CMIP5 Abrupt Event catalogue indicates a positive feedback-driven shift in sea ice state to bimodality, potentially indicating bistable states and hysteresis, but IPCC AR6 has low confidence in SOSI model projections due to significant model limitations in this region.
	EQSC	Equatorial Stratocumulus	6.3	6.3	8.9	10	/	/	8.0	10.0	?	Y	N?	Y	Occurs at 1200+ppm (1400-2200ppm sens. analysis) => 6.3°C (7-8.9°C); only one model so far, so relatively

		us Clouds [breakup]													uncertain; speculated to be involved in high palaeo climate sensitivity for hothouse periods
	AAB W	Antarctic Bottom Water [collapse]	2?	1.8	3.0	50	30	100	?	?	?	M	Y	Y	Uncertain as CMIP models lack Antarctic freshwater melt forcing, so only based on one model and sensitive to e.g. sea ice (which AR6 has low confidence in projections for). SMOC collapse likely to be globally impactful if it occurred though, making it a potential candidate for global core tipping element.
	IOUP	Indian Ocean Upwelling [abrupt increase]	10.9	/	/	25	/	/	<	/	?	M	N	M	Features in CMIP5 Abrupt Event catalogue not only in one model, results in strong productivity increase as a result of a self-amplifying increase in upwelling strength (triggered by increased wind stress & equatorial divergence).
	TIBS	Tibetan Plateau Snow [abrupt loss]	1.8	1.4	2.2	25	/	/	<	+	?	N	N	?	CMIP5 Abrupt Event catalogue indicates abrupt snow loss from Tibetan Plateau passed a threshold (likely due to a threshold mechanism rather than positive feedbacks), but this only occurs in a couple of model runs.
	OCOX	Ocean Oxygenation [global anoxia]	?	/	8.0	10ky	2ky	500 ky	<	/	>1ky	Y	M	Y	Level of warming required to double P weathering (which is theoretically sufficient for a GOAE to eventually develop) is uncertain and most ESMs cannot run long enough for a GOAE to fully develop, but RCP8.5 may be sufficient to more than double P weathering over long enough timescales.
Unlikely to be a Tipping Element	AOZH	Arctic Ozone Hole [abrupt expansion]	N/A	/	/	1	/	/	?	?	?	M	N	N	Only a climate tipping point in combination with CFC emissions (with stratospheric cooling from both global warming & ozone destruction by CFCs triggering further ozone destruction, providing a potential self-perpetuation mechanism). However, due to reversed CFC emissions and ozone layer recovery this is projected to be an insignificant risk by mid 21st Century.
	ENSO	El Nino Southern Oscillation [permanent /extreme]	N/A	3.0	6.0	100	/	/	N/A	?	?	N	N	N	Insufficient evidence for a sharp regime threshold for more extreme or persistent ENSO, though rainfall amplitude variability is projected to increase with warming

	JETI	Northern Polar Jet Stream [instability]	N/A	/	/	?	/	/	N/A	?	?	?	?	?	Insufficient evidence to confirm Arctic amplification - Jet stream instability link, and no evidence yet for a warming threshold driven by tipping dynamics. Only included as a candidate tipping element in Steffen et al. (2018), with no explanation provided as to likely tipping dynamics.
--	------	---	-----	---	---	---	---	---	-----	---	---	---	---	---	---

*Bold = featured in previous climate tipping element characterizations in Table S1

**Global feedback strengths in °C are calculated using ECS and a baseline CO2 corresponding to the central tipping threshold estimate (or pre-industrial for gradual/abrupt permafrost thaw). Feedback strength declines with further degrees of warming (by ~21% per °C). Actual feedback strength for a given warming should be calculated with original GtC emission and then converted to equivalent °C.

***Self-perpetuation, rate-dependence, and hysteresis key: Y = Yes; M = Maybe; N = No; P = Partial; L = Localized; ? = Unknown

Table S5. Table comparing estimated tipping thresholds in past climate tipping element characterizations, CMIP5 abrupt events, and in this assessment. Bold element names are considered a global core element, normal font indicates regional impact elements, and italics indicates uncertain tipping elements, unlikely tipping elements, or threshold-free feedbacks. Colors indicate threshold proximity (red = <2°C, yellow = 2-5°C, green = >5°C).

Proposed Climate Tipping Element [& Tipping Point]	Thresholds in past climate tipping element characterizations (°C)				Thresholds in CMIP5 abrupt events (°C)	Thresholds in this Assessment (°C)
	Lenton et al. (2008)	Schellnhuber et al. (2016)	Steffen et al. (2018)	Lenton et al. (2019)	Drijfhout et al. (2015)	
<i>Arctic Summer Sea Ice [loss] (ASSI)</i>	0.5-2	1-2.6	1-3	2<	Rapid ice melt feedbacks not well represented	2.0 (1.3-2.9)
Greenland Ice Sheets [collapse] (GrIS)	1-2	1-3.2	1-3	1.5		1.5 (0.8-3.0)
West Antarctic Ice Sheet [collapse] (WAIS)	3-5	1-5.6	1-3	1-1.5		1.5 (1.0-3.0)
Atlantic M.O. Circulation [collapse] (AMOC)	3-5	3.5-5.6	3-5	N/A	1.6*	4.0 (1.4-8.0)
Amazon Rainforest [dieback] (AMAZ)	3-4	3.5-4.6	3-5	N/A	2.5 / 6.2	3.5 (2.0-6.0)
Boreal Forest [southern dieback] (BORF)	3-5	3.5-5.6	3-5	N/A	Limited veg. dynamics	4.0 (1.4-5.0)
Boreal Permafrost [collapse] (PFTP)	N/A	4.8-9+	5+	N/A	5.6	4.0 (3.0-6.0)
Sahel & W. African Monsoon [greening] (SAHL)	3-5	3.5-5.6	3-5	N/A	2.8	2.8 (2.0-3.5)
<i>El Niño [permanent/extreme] (ENSO)</i>	3-6	3.5-6.6	3-5			N/A (3.0-6.0)
Low-latitude Coral Reefs [die-off] (REEF)		1.3?-1.8?	1-3	<2	Not represented	1.5 (1.0-2.0)
East Antarctic Ice Sheet [collapse] (EAIS)		4.5-9+	5+		Timescale not modelled	7.5 (5.0-10.0)
Arctic Winter Sea Ice [collapse] (AWSI)		5.5-9+	5+		6.3	6.3 (4.5-8.7)
Extra-polar Mountain Glaciers [loss] (GLCR)		1-2.6	1-3			2.0 (1.5-3.0)
<i>Northern Polar Jet Stream [instability] (JETS)</i>			3-5			N/A
<i>Indian Summer Monsoon [collapse] (INSM)</i>	N/A		3-5	N/A		N/A (only if AMOC)
<i>Ocean Oxygenation [global anoxia] (OCOX)</i>	N/A					? (<8.0)
<i>Arctic Ozone Hole [abrupt expansion] (AOZH)</i>	?					N/A
<i>Antarctic Bottom Water [collapse] (AABW)</i>	?					2? (1.8-3.0)
<i>Marine Methane Hydrates [dissoc.] (MMHD)</i>	?		N/A			2.0?
Boreal forest [northern expansion] (TUND)	N/A				7.2	4.0 (1.5-7.2)
<i>Southern Ocean sea ice [bimodality] (SOSI-Bi)</i>					2.9	2.9 (1.7-4.5)
<i>Indian Ocean upwelling [increase] (IOUP)</i>					10.9	10.9
Barents sea ice [loss] (BARI)					1.6	1.6 (1.5-1.7)
<i>Southern Ocean sea ice [loss] (SOSI-AP)</i>					2.1	2.1 (1.4-2.9)
<i>Southern Ocean sea ice [increase] (SOSI-In)</i>					1.6	1.6
Labrador Sea /SPG Convection [collapse] (LABC)					1.7	1.9 (1.5-3.8)
<i>Tibetan Plateau Snow [abrupt loss] (TIBS)</i>					1.8	1.8 (1.4-2.2)
<i>Equatorial Stratocumulus Clouds [breakup] (EQSC)</i>				1200ppm		6.3 (6.3-8.9)
<i>Ocean Biological Pump [weaken] (PUMP)</i>			N/A			N/A
<i>Global Land Carbon Sink [weaken] (LAND)</i>			N/A			2.0 (1.0-3.5)

*Likely too low

Data S1 (separate file). Database containing details of the full literature assessment used to summarize estimates for climate tipping thresholds, timescales, impacts, and dynamics. The spreadsheet includes a summary of past climate tipping element characterizations (sheet 1), abrupt events detected in CMIP5 by Drijfhout et al. (2015) (sheet 2), key tables from recent IPCC reports concerning tipping points (sheet 3), our summary estimates for each proposed climate tipping element (sheet 4), our estimated thresholds compared with previous characterizations (sheet 5), the detailed analysis of each reference our estimates are based on (sheet 6), and estimates of regional temperature-mediated interactions between selected tipping elements (sheet 7).